UC Berkeley
UC Berkeley Previously Published Works

Title

What are the effects of Agro-Ecological Zones and land use region boundaries on land resource projection using the Global Change Assessment Model?

Permalink

https://escholarship.org/uc/item/0sc1740q

Authors

Di Vittorio, AV
Kyle, P
Collins, WD

Publication Date

2016-11-01

DOI

10.1016/j.envsoft.2016.08.016

Peer reviewed

What are the effects of Agro-Ecological Zones and land use region boundaries on land resource projection using the Global Change Assessment Model?

Alan V. Di Vittorio[a,*], Page Kyle[b], and William D. Collins[a,c]

[a]Lawrence Berkeley National Laboratory
Climate and Ecosystems Sciences Division
One Cyclotron Road, MS 74R316C
Berkeley, CA 94720-8268

[b]Joint Global Change Research Institute
Pacific Northwest National Laboratory
5825 University Research Court
Suite 3500
College Park, MD 20740

[c]University of California, Berkeley
Department of Earth and Planetary Sciences
307 McCone Hall
Berkeley, CA 94720-4767

[*]Corresponding author
avdivittorio@lbl.gov, Tel.: +1-510-486-7798

Abstract

Understanding potential impacts of climate change is complicated by spatially mismatched land representations between gridded datasets and models, and land use models with larger regions defined by geopolitical and/or biophysical criteria. Here we quantify the sensitivity of Global Change Assessment Model (GCAM) outputs to the delineation of Agro-Ecological Zones (AEZs), which are normally based on historical (1961-1990) climate. We reconstruct GCAM's land regions using projected (2071-2100) climate, and find large differences in estimated future land use that correspond with differences in agricultural commodity prices and production volumes. Importantly, historically delineated AEZs experience spatially heterogeneous climate impacts over time, and do not necessarily provide more homogenous initial land productivity than projected AEZs. We conclude that non-climatic criteria for land use region delineation are likely preferable for modeling land use change in the context of climate change, and that uncertainty associated with land delineation needs to be quantified.

Keywords

Highlights

- Land resource inputs and projections are sensitive to land use region boundaries.
- Developed a system to generate land data for given Agro-Ecological Zones (AEZs).
- AEZs based on projected climate differ considerably from historical AEZs.
- Climate within historical AEZs becomes spatially heterogeneous with climate change.
- Non-climatic land use region boundaries may reduce model error, compared to AEZs.

1. Introduction

Global climate projections rely on a scenario-based process by which Integrated Assessment Models (IAMs) generate estimates of anthropogenic emissions and spatially explicit land use change for driving global climate and Earth System Models (ESMs) (Moss et al., 2010; Taylor et al., 2012, van Vuuren et al., 2014). These projections are used in turn to estimate impacts of global change on a wide variety of human and environmental systems. Climate change in the upcoming century is expected to substantially change conditions at local and regional scales, but current assessments indicate a high degree of variability in impact direction and magnitude across models, regions, and sectors (IPCC, 2014a). Some of this variability may be due to uncertainty in regional climate projections. For example, recent studies have highlighted large spreads in regional multi-model climate ensemble projections, at both coarse and fine resolutions (e.g., Mearns et al., 2013; Qiao et al., 2014, van der Linden and Mitchell, 2009). While these differences are often attributed to model differences in general, inappropriate resolution or spatial aggregation in models can cause significant biases in outputs (Di Vittorio and Miller, 2014; Ogle et al., 2006; Riley et al., 2009).

Unfortunately, uncertainties associated with a given spatial delineation of the earth are not usually accounted for in modeling studies because models are often constructed at only a single resolution or level of aggregation, or because it is too computationally expensive to rerun simulations using different spatial configurations. Errors associated with a given spatial delineation are compounded when different models interact, as is the case in scenario-based global climate projections. Where IAMs often delineate the earth based on geopolitical and biophysical factors, ESMs generally use a regular grid at coarse resolution, and impact models usually have fine resolution with either regular or irregular grids. Not only are the spatial units different between models, but the types and definitions of land use and cover are different as well. These fundamental discrepancies and associated inconsistencies in the IAM-ESM-impact chain can render projections of local and regional climate change and impacts invalid, and in some cases cause ESMs to simulate an entirely different scenario from the one prescribed by the IAM (Di Vittorio et al., 2014).

Four IAMs, each with a different spatial delineation of the land surface, generated the four Representative Concentration Pathway (RCP) scenarios (van Vuuren et al., 2011a) used by ESMs in phase 5 of the Coupled Model Intercomparison Project (CMIP5) (Taylor et al., 2012). RCP class IAMs are economic models that project detailed breakdowns of the production and use of energy and land resources, balancing supplies and demands of modeled commodities through market mechanisms. A key feature of these IAMs is that they include a biogeophysical component that estimates climate change associated with projected energy and land resource utilization. This interaction between the human and

environmental components is critical for generating the RCP scenarios, which are based on specific climate targets (van Vuuren et al., 2011a), although climate impacts are not fed back into energy and land projections. Incorporating the climate-land feedbacks using mechanistic ecosystem models is a relatively new area of research (Calvin et al., 2013; Di Vittorio et al., 2014; Kicklighter et al., 2014; Kyle et al., 2014; Reilly et al., 2012) and has the potential to introduce additional uncertainty associated with model spatial delineations.

For CMIP5, each IAM calculated land use for a different set of geopolitical regions, and these outputs were harmonized to historical data by a separate model with its own unique representation of land use. The four IAM models contain the following numbers of regions: 11 (MESSAGE, Riahi et al., 2011), 14 (GCAM, Thomson et al., 2011), 24 (AIM, Masui et al., 2011), and 26 (IMAGE, van Vuuren et al., 2011b). Three models (AIM, MESSAGE, IMAGE) incorporated downscaling to a half-degree grid, with MESSAGE and IMAGE using historical Agro-Ecological Zone (AEZ) data to inform the downscaling. The individual model outputs were harmonized (and downscaled in the case of GCAM) by the Global Land-use Model (GLM) to a half-degree global grid (Hurtt et al., 2011), and then passed to ESMs. GLM employs local spatial relationships, but as a global model it still lacks local constraints such as barriers to land availability, limits to intensification, (in)accessibility to markets, restrictions on land use practices, and land governance and tenure (Verburg et al., 2013). Regardless, the land use harmonization process propagated uncharacterized spatial error unique to each IAM due to different sensitivities to the land regions delineated by each model.

The modeled land regions and corresponding initial state of these IAMs critically determine their land resource projections, and require a tremendous amount of data to ensure proper calibration to present day conditions. Model goals generally determine the type of land use model, and combined with available data, also the extent and resolution (Brown et al., 2013). IAMs have traditionally represented human activities in 10-30 geopolitical regions due to their origins as energy market models, and some of these models have recently disaggregated their geopolitical regions into smaller units for land use modeling, often using historical AEZs as the basis for this disaggregation (e.g., Schmitz et al, 2014). AEZs have been used in land use modeling for decades (e.g., Fischer et al. 1996; for review see FAO 2016) to improve the real-world feasibility of modeled land use transitions by taking advantage of similarities in climate, soil, and topography (Lee et al., 2005). The use of AEZs to disaggregate geopolitical regions in IAMs also refines the spatial resolution of land use regions, and allows more detailed estimation of physical characteristics that are relevant for model outcomes (e.g., crop productivity, vegetation types, carbon contents). However, generating the IAM-relevant data associated with these AEZs is a major task.

A set of commonly used historical AEZs and associated land data were developed by the Global Trade Analysis Project (GTAP; Monfreda et al. 2009), and models that currently use this particular set of AEZs to disaggregate geopolitical regions include AIM (Hasegawa et al. 2015), FARM (Sands et al. 2014), GCAM (http://www.globalchange.umd.edu/archived-models/gcam/), and GTAP-AEZ (Hertel et al. 2009), among others. BLS-AEZ (Fischer et al. 2005) also uses similar terminology for classifying land, but with different criteria and sub-regional zone boundaries than the GTAP AEZs. However, the traditional IAM modeling paradigm does not include climate impacts, leaving an unexplored question regarding the representativeness of AEZ-averaged values in land use modeling under changing climate, in which case the AEZs may not retain their expected homogeneity. Note that the use of AEZs is not ubiquitous in land use modeling; other strategies to disaggregate geopolitical regions using primarily non-climatic criteria include grid cell boundaries (e.g., MAgPIE, Dietrich et al. 2014; GLOBIOM, Havlik et al., 2013), hydrologic watersheds (e.g., IMPACT, Rosegrant et al. 2012), and province/state boundaries (e.g., FASOMGHG, Beach et al. 2015). While these non-climatic boundaries avoid some issues associated with AEZs in the context of climate change, they can still suffer from lack of representativeness if they are not carefully defined, and they still generate model uncertainty associated with a particular delineation of the land surface.

Here we quantify the uncertainty in land resource projection due to spatial delineation of the land surface using the Global Change Assessment Model (GCAM), which is a community IAM that has been, and continues to be, used to generate scenarios for international climate assessments (van Vuuren et al., 2011a). While we use the AEZ methodology as implemented in GCAM, the present study is not an investigation of the effectiveness of current methods for representing agricultural climate impacts in land change models, nor is it an attempt to develop a new method of climate impacts assessment. Rather, we aim to 1) determine whether climatically defined boundaries, in particular AEZs, are appropriate in a land modeling context, and 2) characterize and quantify uncertainty in land resource projection due to spatial delineation of the land surface. To address these aims we generate new spatial boundaries (Section 3.1), evaluate the suitability of AEZ-based data sets for land use modeling under climate change (Section 3.2), quantify differences in inputs (Section 3.3) and outputs (Sections 3.4) due to different land use regions, and discuss the implications of these differences for land use modeling with and without climate impacts (Section 3.5).

2. Methods

GCAM is a community IAM that simultaneously represents human and biogeophysical processes associated with climate change (http://www.globalchange.umd.edu/archived-models/gcam/).

The human system simulates activities within the global energy, industrial, and agricultural systems that are relevant for producing emissions and changing land use patterns. The biogeophysical system simulates feedbacks with the carbon cycle and the resulting impacts on the atmosphere and climate. A comprehensive data processing system generates GCAM input files from a wide variety of source data spanning resolutions from 5 arcmin grid cells to the globe.

To facilitate projection of both energy and land resources, GCAM contains two distinct modules—energy, and Agriculture and Land Use (AgLU)—that are linked via markets for bioenergy, nitrogen fertilizer, and (where applicable) greenhouse gas emissions. The AgLU component models land use decisions at scales that are smaller than the geopolitical regions at which markets for agricultural and energy goods are modeled. The intersection of 18 global AEZs with the geopolitical regions defines the land use regions in the AgLU module. The purpose of these smaller land use regions is to represent the heterogeneity in land productivity that exists across environmentally diverse geopolitical regions.

Our first goal is to determine the suitability of AEZs for splitting geopolitical regions into smaller land use regions. Each AEZ represents particular bioclimatic conditions as defined for a given time period. This means that temperature and water availability regimes are assumed to be relatively similar throughout each AEZ, allowing for the modeling assumption that average crop and vegetation productivity is representative of an entire AEZ. A major challenge to this approach is that the AEZs are defined only for 1961-1990 bioclimatic conditions, but the level of land and energy resource utilization in most IAM scenarios is expected to cause climate change over the 21st century (IPCC, 2014b). Actual AEZ boundaries will shift due to climate change as temperature and water availability change, causing the original land use regions to experience potentially heterogeneous rates of change that could lessen accuracy in determining the environmental conditions relevant for future crop production. To facilitate further exploration of the effects of bioclimatic heterogeneity in projections, we determine new land use regions by defining a new set of AEZs based on a realization of 2071-2100 climate.

Our second goal is to quantify the sensitivity of land resource projections to the land use region boundaries. This is a necessary first step toward examining the combined effects of spatial structure and aggregated climate impacts on projections. Given the difficulty of changing the model structure to accommodate a new spatial configuration, and the potential for using projected AEZs to better understand the limitations of such approach under climate change, we have elected to use the projected AEZs from our first goal as the new boundaries for assessing spatially driven uncertainty in GCAM. It is important to note that we do not impose climate change impacts in this study, which is consistent with CMIP5 (van Vuuren et al., 2011a) and the upcoming CMIP6 (O'Neill et al., 2014), for which climate impacts are not included in climate and socio-economic pathway generation. Omitting climate impacts

avoids confounding our analysis with averages of temporally and spatially heterogeneous impacts. Furthermore, the distributions of circa year-2000 individual crop yields (Monfreda et al., 2008) within GCAM land use regions are not any more homogenous for the historical AEZs than for the projected AEZs (Figure 1), indicating that the AEZ method does not necessarily provide the homogeneity of land productivity assumed by the land use projection algorithm. This indicates that there is no clear advantage to one set of boundaries over the other, and allows us to use the projected AEZs as an independent, alternative boundary set in assessing the uncertainty associated with the spatial configuration of the model.

In order to evaluate AEZ suitability and carry out the required GCAM simulations (section 2.1), we have generated new AEZ boundaries defined by climate projections for the end of the 21st century (section 2.2) and implemented a Land Data System (LDS) that generates new inputs to the GCAM data processing system for any given set of AEZ boundaries (section 2.3). The LDS output replaces certain data system inputs (Table 1) in order to initialize GCAM's (AgLU) module with the projected set of AEZs. Additionally, the raster image of the AEZ boundaries (section 2.2) is a primary input to the geographic preprocessing system that provides tabular data for input to the comprehensive data system.

Figure 1. Comparison of circa year-2000, individual crop yield variation within GCAM land use regions. Using New (projected) versus Original (historical) AEZ boundaries has a negligible effect on the spread of individual crop yields within the regions. Each value included in these histograms represents one of 175 crops, where present, within each of 151 land use regions.

a) Standard deviation distribution comparison

b) Coefficient of variation distribution comparison
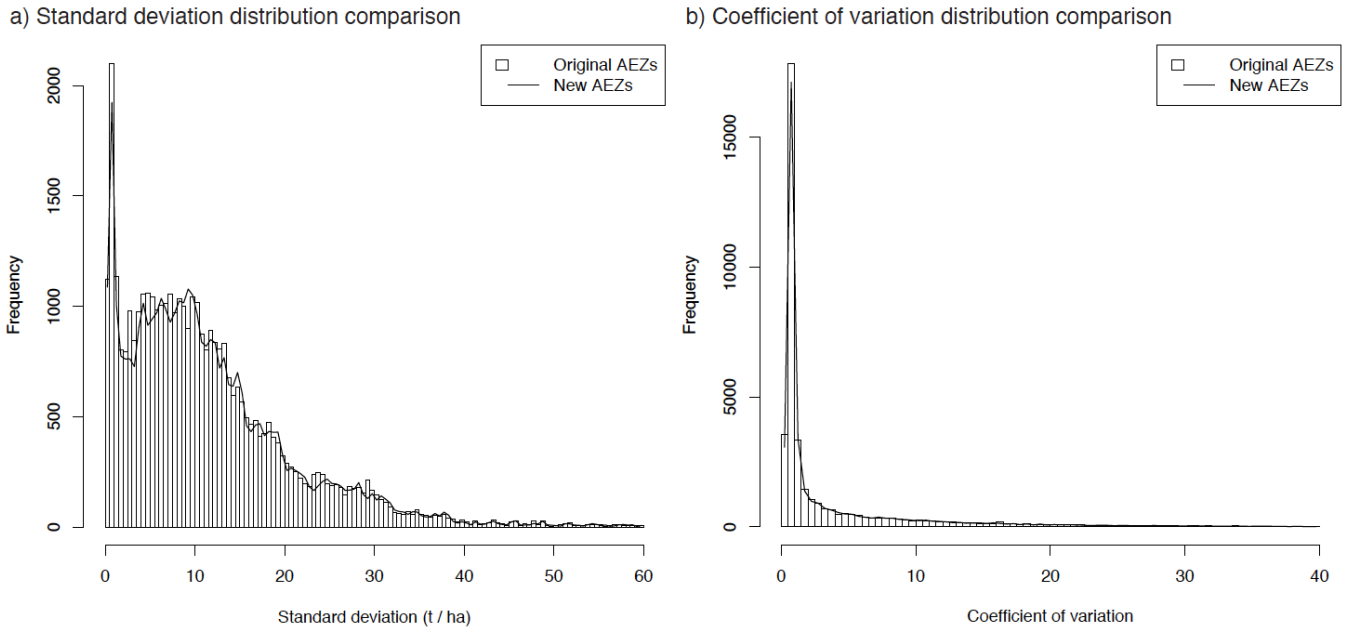
2.1. GCAM simulations

We run two reference scenario simulations from 2010 – 2100 at 5-year time steps, with 2010 designated as the base-year for calibration and reporting purposes. The reference scenario in GCAM has been documented elsewhere (e.g., Eom et al. 2013), and in the context of ongoing scenario development in integrated assessment models, its assumptions are similar to the "middle of the road" SSP2 pathway (O'Neill et al. 2015). As with SSP2, global population peaks in about 2070, and per-capita incomes increase in all regions throughout the course of the century, with particularly high rates of growth assumed in currently developing nations. Of particular relevance for agriculture and land use, global average per-capita caloric demands increase by 6% from 2010 to 2100, with 15% growth in animal product caloric demands. Furthermore, purpose-grown second-generation bioenergy crop demands increase from 0 in the base year to between 50 and 70 EJ per year by mid-century. No climate impacts are applied in these scenarios.

For this study, we remove all AEZ-dependent assumptions from GCAM in our simulations. By default, the potential locations and types of biomass crops for energy and the carbon densities assumed for several ecosystem types are specified by AEZ. That is, in several minor instances, the AEZ number is used to infer characteristics about the land and its potential uses. In order to avoid any interactions

between these model assumptions and the AEZ boundaries, we have restricted biomass to a single crop and allowed it to be introduced in all land use regions, and we have used carbon density values that do not vary by AEZ. These carbon densities are used to calculate land use change emissions and to determine the proportion of forest harvested for wood products. For each land type we use an average of the default carbon values, which were derived from several literature sources as documented in Kyle et al. (2011).

We perform two simulations using the assumptions above with: 1) original AEZ input data as generated by the LDS and 2) new AEZ input data as generated by the LDS. The only difference between these two simulations is that they use different land use region boundaries for initialization (Table 1) and projection of land resources.

Our GCAM output analysis focuses on simple differences in land resource outputs between the original and new AEZ simulations. We calculate these differences for each region and for the globe, and present them as percent change relative to the original AEZ outputs.

Table 1. Initialization data replaced to run GCAM with new Agro-Ecological Zone (AEZ) boundaries. See Tables 2 and 3 for source data.

Description	Update method	Used by
Agricultural harvested area and production of 175 crops for each AEZ within 226 countries	Land Data System	GCAM data processing system
Total land rent value of 12 commodity sectors for each AEZ within 87 regions	Land Data System	GCAM data processing system
Association of each AEZ with a country	Land Data System	GCAM data processing system
Association of each grid cell with an AEZ, country, and GCAM region	Land Data System	Geographic preprocessing
Raster image of AEZ areas	R script	Geographic preprocessing

2.2. AEZ boundaries

The original AEZ boundaries are provided by the Global Trade Analysis Project version 6.0 Land Use Data set 2.1 (henceforth referred to as GTAP; Lee et al., 2005; Lee et al., 2009; Monfreda et al., 2009). They have been derived from a combination of Global AEZ (GAEZ) version 1.0 length of annual growing period data (Fischer et al., 2002) and other climate data for the baseline period of 1961-1990 (Ramankutty and Foley, 1999). We implement the GTAP methods (Lee et al., 2005; Monfreda et al., 2009) in an R script (www.r-project.org) to generate a new global AEZ image file at 5 arcmin resolution, based on a realization of 2071-2100 climate, as described below (also see Figure 2).

2.2.1. Boundaries data

The input data required to generate new AEZ boundaries come from multiple sources, detailed in Table 2. The original AEZ image is used to mask all other data so that the new AEZ image is an exact geographic match, except for the new AEZ boundaries. The future length of growing period data are from the GAEZ version 3.0 database (Fischer et al., 2002; IIASA/FAO, 2012) and use downscaled, 2071-2100, ECHAM4 climate model (Roeckner et al., 1996) output for the A2 scenario of the Special Report on Emissions Scenarios (SRES) (IPCC, 2000). Downscaled SRES A2, ECHAM5 (Roeckner et al., 2003), maximum and minimum monthly temperature averaged over 2081-2090 (Jones et al., 2009), combined with daily minimum temperature from 1961-1990 (Adam and Lettenmaier, 2003; Maurer et al., 2009) and monthly minimum temperature averaged over 1961-1990 (Hijmans et al., 2005), are used to delineate the three temperature zones. While the averaging periods and model versions do not exactly match, these are the only available relevant data, and we have been fortunate enough to find suitable climate data that matches closely with the source data for the length of growing period calculation.

Table 2. Data inputs for defining new Agro-Ecological Zone (AEZ) boundaries.

Data	Details	Source[a]
Original AEZ boundaries	5 arcmin, 1961-1990 data, 160 country boundaries	Lee et al., 2005; Lee et al., 2009; Monfreda et al., 2009; https://www.gtap.agecon.purdue.edu/resources/res_display.asp?RecordID=1900
Average length of annual growing period	5 arcmin, 2071-2100 average, SRES A2 scenario, ECHAM4 model	Fischer et al., 2002; IIASA/FAO, 2012; http://www.fao.org/nr/gaez/en/
Average monthly minimum and maximum temperature	5 arcmin, 2081-2090 average, SRES A2 scenario, ECHAM5 model	Jones et al., 2009; http://www.ccafs-climate.org/data/
Daily minimum temperature	0.5°, 1961-1990	Adam and Lettenmaier, 2003; Maurer et al., 2009; http://www.engr.scu.edu/~emaurer/global_data/
Average monthly minimum temperature	5 arcmin, 1961-1990 average	Hijmans et al., 2005; http://www.worldclim.org/current

[a]All these data were accessed in late 2012.

2.2.2. Boundaries processing

The 18 global AEZs are created by intersecting six, length of annual growing period bins with three temperature zones (Ramankutty and Foley, 1999; Lee et al., 2005; Monfreda et al., 2009). The length of growing period is calculated for each grid cell using climate, soil, and reference grass data (Fischer et al., 2002; IIASA/FAO, 2012). A day is included in the growing period if the average daily temperature is greater than 5°C and the actual evapotranspiration is greater than or equal to half of the potential evapotranspiration. The first five growing period bins each include 60 days while the sixth bin includes days greater than or equal 300. The length of growing period generally relates to moisture regime, with the shortest being dry and the longest being humid, but in some places the daily average temperature determines the growing period bin.

The temperature zones are derived from a combination of annual Growing Degree Days (GDD) (°C); 5°C base):

$$GDD = \sum_{d=1}^{365} \frac{\max(t_{max}, 30) + \min(t_{min}, 5)}{2}, \qquad (1)$$

where t_{max} is the daily maximum temperature, t_{min} is the daily minimum temperature, and d is the day of year, and the absolute minimum daily temperature over the period of interest, following these rules:

a) Hot: absolute minimum temperature > 0 °C

b) Temperate: absolute minimum temperature > -45 °C and GDD > 1200 °C

c) Cold: everywhere else

The intersection of growing period and GDD data delineates 18 zones with zones 1-6 being hot, 7-12 temperate, and 13-18 cold. Within each temperature zone the lowest number is the shortest length of growing period and the highest number is the longest (Lee et al., 2005; Monfreda et al., 2009).

We transform our average monthly data to produce daily values required by the GDD and temperature zone calculations. Average monthly temperature values are applied to each day of each month to calculate the average annual GDD over 2081-2090. To estimate the absolute minimum temperature for the 2081-2090 temperature data, we first calculate the difference between average monthly minimum temperature (averaged to half-degree) and the absolute daily minimum temperature within each month for 1961-1990. We calculate this difference at half-degree resolution, and then subtract it via disaggregation from the 2081-2090 average monthly minimum temperature data. The minimum value across months for each grid cell is used as the absolute minimum temperature for determining the temperature zone.

We calculate differences between the new and original thematic AEZ data sets to examine the spatial patterns of changes in length of growing period, temperature zone, and AEZ in relation to the original GCAM land use regions.

2.3. AEZ land data

GTAP provides the original land data for each AEZ within each country or region. The three primary land variables used to initialize GCAM are crop production, crop harvested area, and land rent value. The crop data are provided for 175 crops in 226 countries, and the land rent data for 13 agricultural sectors in 87 countries and regions. Here we implement the GTAP methods (Lee et al., 2005; Lee et al., 2009; Monfreda et al., 2009) in our LDS to recalculate these initial data for both the original (section 2.2) and new (section 2.2.2) AEZ boundaries.

2.3.1. Land data

A wide variety of source data are required to generate the production, harvested area, and land rent data provided by GTAP (Table 3). A major challenge to reproducing the original GTAP data is that the spatially explicit data (i.e., raster and vector data) are independent of the tabular data (e.g., crop production listed by country). This makes it unlikely that our LDS will aggregate the source gridded data to the exact same country boundaries used for the original GTAP data. Additionally, four different country sets require reconciliation among the source data, further decreasing the fidelity between LDS and the original GTAP data.

The primary source data are globally gridded maps of circa year-2000 yield and harvested area for 175 crops (Monfreda et al., 2008), and are the same for LDS and GTAP (see Monfreda et al., 2009). These data, combined with the country and AEZ boundaries, determine the initial crop production and harvested area for the GCAM data processing system. These data include fodder crops, including fodder grasses that are used to determine the yield of intensive pasture for ruminant production in GCAM.

The remaining source data, used for calculating land rent, are not exactly the same between LDS and GTAP. For example, we combine global cropland and pasture area (Ramankutty et al., 2008) with HYDE3.1 urban area (Klein Goldewijk et al., 2010) and potential vegetation data (Ramankutty and Foley, 1999) to determine forest and pasture area for calculating forestry and livestock land rents, while GTAP additionally used outputs from a biome model (Haxeltine and Prentice, 1996) and a timber model (Sohngen et al., 1999) to further disaggregate forest and management types (Lee et al., 2005, Lee et al., 2009). We do not use these additional data because not all the required data and metadata are available. It is also possible that we used different Food and Agriculture Organization (FAO) crop production and price data than GTAP for calculating agricultural land rents because we downloaded these data several years after GTAP. We do, however, use the GTAP sector land rent data, aggregated to the 87-region level, as the starting point for disaggregating land rent to given AEZ boundaries.

Table 3. Land Data System (LDS) inputs for calculating land data for Agro-Ecological Zone (AEZ) boundaries.

Data	Details	Source[a]
Crop yield and harvested area	5 arcmin, 175 crops-same as GTAP, circa 2000, area provided as fraction of land area in grid cell	Monfreda et al., 2008; http://www.sage.wisc.edu/mapsdatamodels.html
Cropland extent and pasture area	5 arcmin, circa 2000, provided as fraction of land area in grid cell	Ramankutty et al., 2008; http://www.sage.wisc.edu/mapsdatamodels.html
Fraction of land area in grid cell	5 arcmin, spherical earth. average WGS84 radius	D. Plouff and N. Ramankutty provided these data corresponding to the above crop and pasture data (in late 2013)
Potential vegetation	5 arcmin, thematic, vegetation circa 2000 if no historical land use had occurred	Ramankutty and Foley, 1999; http://www.sage.wisc.edu/mapsdatamodels.html
Urban area	5 arcmin, circa 2000	Klein Goldewijk et al., 2010; http://themasites.pbl.nl/tridion/en/themasites/hyde/download/index-2.html
Land area in grid cell	5 arcmin, for urban area fraction, excludes glaciers	Klein Goldewijk et al., 2010; http://themasites.pbl.nl/tridion/en/themasites/hyde/download/index-2.html
Total grid cell area	5 arcmin, for urban area fraction	Klein Goldewijk et al., 2010; http://themasites.pbl.nl/tridion/en/themasites/hyde/download/index-2.html
246 Country boundaries	5 arcmin, from VMAP0 vector data (the source of FAO	VMAP0: http://gis.ess.washington.edu/data/raster/GlobalData/

	country boundaries), added East Timor from the Timor-Leste Geographic Information Group	East Timor: https://sites.google.com/site/gigtimorleste/home
Original AEZ boundaries	5 arcmin, 1961-1990 data, 160 country boundaries	Lee et al., 2005; Lee et al., 2009; Monfreda et al., 2009; https://www.gtap.agecon.purdue.edu/resources/res_display.asp?RecordID=1900
GTAP 226 countries and 87 regions	Tabular	Lee et al., 2005; Lee et al., 2009; Monfreda et al., 2009; https://www.gtap.agecon.purdue.edu/resources/res_display.asp?RecordID=1900
Land rent for 13 use sectors	Tabular, 87 regions by 18 AEZs, original GTAP data	Lee et al., 2005; Lee et al., 2009; Monfreda et al., 2009; https://www.gtap.agecon.purdue.edu/resources/res_display.asp?RecordID=1900
FAO 241 countries	Tabular	Jones et al., 2009; http://www.ccafs-climate.org/data/
FAO Crop production and producer prices	Tabular, up to 169 crops	http://faostat.fao.org/; accessed Aug 2013

[a]All these data were accessed in late 2012 unless otherwise noted.

2.3.2. Land processing

We use the LDS, as described below, to generate production, harvested area, and land rent data for both the original and new AEZ boundaries. The LDS outputs are in the tabular format used by the GCAM data processing system. The bulk of the processing reconciles inconsistencies among all the input data sets. The final outputs are based on data that are in a valid AEZ grid cell, as determined by the original AEZ image file, and also in a cell with land area, as determined by the land fraction data. Assignment of raster data to countries is based on a combination of the 246-country boundary data and the original AEZ image file. The 246-country boundary data is also used by the FAO, and so LDS uses

these 246-country data first to assign a cell to a country. If a country is not found for a given cell, then the country in the original AEZ image file is used. The cell data are not used if no country can be associated with it. These spatial countries are mapped to the tabular GTAP and FAO countries for further processing of the data, causing the raster data to be aggregated in some cases (e.g., Serbia and Montenegro) and omitted in others (e.g., GTAP does not include Western Sahara). The non-agricultural land cover is determined by assigning the potential vegetation to the non-crop/pasture/urban land in each grid cell. The land fraction data, combined with the assumption of a spherical earth, determine the land area within a grid cell because they are consistent with the 175-crop, total cropland, and total pasture data. The HYDE urban area are reconciled with the other land type data through conversion to fraction of land area within the grid cell, and then back to area using the land fraction data. If the land area is less than the total crop, pasture, and urban area, then first urban, then pasture, and then crop area are reduced until their total matches the land area.

Once these data are reconciled, the crop production and harvested area for each crop in each AEZ in each GTAP country are determined from the gridded 175-crop yield and harvested area data. There are 226 GTAP countries, and not every crop or AEZ are present in each country. Harvested area and production (harvested area multiplied by yield) are simply summed across all grid cells within a given boundary because the source data have already been normalized to 1997-2003 average annual FAO data (Monfreda et al., 2008; Monfreda et al., 2009).

The agricultural and forestry land rent data are generated separately at the level of 87 regions. There are 12 agricultural sectors, including three livestock sectors for meat, dairy, and fiber production, and a non-ruminant livestock sector that has zero land rent value because it is assumed to not use substantial area in production. For each region, the eight crop land rents are distributed among the AEZs following (Lee et al., 2005; Lee et al., 2009):

$$L_{c,a} = L_c \left[\sum_{i \in SECTOR=c} P_i Q_{i,a} \Big/ \sum_{a \in AEZ} \sum_{i \in SECTOR=c} P_i Q_{i,a} \right],$$

(2)

where $L_{c,a}$ is the land rent for sector c in AEZ a (2001USD), L_c is the original total land rent of sector c within a region, P_i is the FAO production-weighted 1997-2003 annual average price per metric ton of GTAP crop i, $Q_{i,a}$ is the production for GTAP crop i in AEZ a (metric tons, from above), $SECTOR$ is the set of GTAP sectors within a region, and AEZ is the set of AEZs within a region.

The livestock sector land rent calculation for each region uses the average cereal grain sector price and yield along with the pasture area, and the proportion assigned to each AEZ is the same for each livestock sector. Using the production-weighted price and the area-weighted yield (from production

16

divided by harvested area above) essentially scales the value term in eq. (2) by the ratio of pasture area
to total harvested grain area within an AEZ:

$$
L_{l,a} = L_l \left[\frac{A_{pasture,a}}{\sum\limits_{i \in SECTOR=grain} A_{i,a}} \sum\limits_{i \in SECTOR=grain} P_i Q_{i,a} \middle/ \sum\limits_{a \in AEZ} \left(\frac{A_{pasture,a}}{\sum\limits_{i \in SECTOR=grain} A_{i,a}} \sum\limits_{i \in SECTOR=grain} P_i Q_{i,a} \right) \right], \quad (3)
$$

where $L_{l,a}$ is the land rent for livestock sector l in AEZ a (2001USD), L_l is the original total land rent of
livestock sector l, $A_{pasture,a}$ is the pasture area in AEZ a, $A_{i,a}$ is the harvested area of GTAP crop i in AEZ
a, *grain* denotes the grain sector, and P_i, $Q_{i,a}$, *SECTOR*, and *AEZ* are the same as in eq. (2).

The forestry land rent within each region is distributed among new AEZs based on the original
land rent per forest area within the original AEZs. First, the original land rent per unit forest area is
calculated for each original AEZ and region. Next, the new AEZ forestry land rent is calculated as the
sum of the product of original land rent per area and forest area within the new AEZ:

$$
L_{f,new} = \sum\limits_{a \in AEZ \cap new} LD_{f,a} A_{f,a \cap new} , \quad (4)
$$

where $L_{f,new}$ is the forest sector f land rent for AEZ *new*, $LD_{f,a}$ is the forest land rent per unit area in
original AEZ a, $A_{f,a \cap new}$ is the forest area of original AEZ a within new AEZ *new*, and AEZ_{orig} is the set
of original AEZs within the region. We cannot reproduce the original method because some of the
required source data and metadata are not available (see Section 2.3.1).

To validate the LDS, we compare the reproduced original AEZ LDS outputs against the original
GTAP data set and FAO, at the country level. We also compare the new AEZ LDS outputs with GTAP
and the reproduced original AEZ LDS outputs at the land use region level to determine how the different
boundaries affect the input data for GCAM. Differences among the data sets are visualized by
cumulative distribution functions and difference histograms derived from values associated with each
defined land use region. We also calculate the mean of the crop- and use-specific regression parameters
among LDS and GTAP outputs at the country and land use region levels.

Figure 2. The Land Data System (LDS). Creation of the Agro-Ecological Zone (AEZ) raster data, shown in the dashed box, is implemented separately from the LDS. The dotted lines separate the three main LDS components. Crop data are processed first because production and harvested area are needed for agricultural land rent. Forestry land rent is independent of the agricultural calculations. Ovals are 5 arcmin raster data, hexagons are tabular data, boxes are processes, and the LDS outputs are in underlined, bold lettering within bold hexagons. GTAP = Global Trade Analysis Project, FAO = Food and Agriculture Organization.
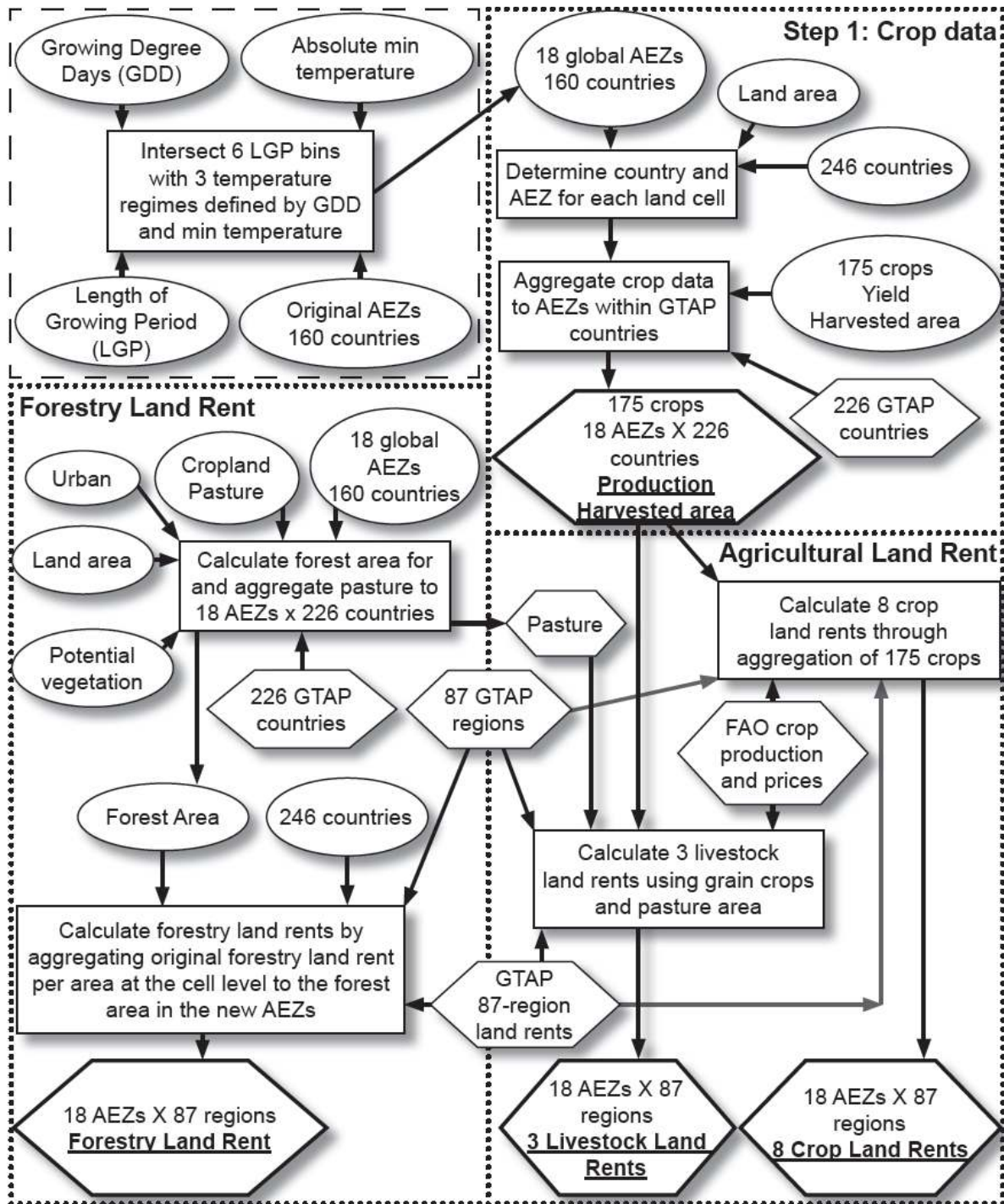
3. Results and Discussion

Using end-of-century climatic conditions to define AEZs dramatically changes the boundaries, and in some cases the size, of the land use regions, which leads to different long-term regional and global land resource outcomes in GCAM. The changes in these boundaries also indicate that climate-related impacts within original land use regions will be spatially heterogeneous. This heterogeneity invalidates the agro-economic modeling assumption that average land productivity is consistent within an entire land use region, thus introducing an additional source of uncertainty that could be exacerbated by averaging climate impacts within these regions.


3.1. New AEZ boundaries

The new AEZs indicate that geographic AEZ shifts are dominated by changes in length of growing period combined with warming in northern high latitudes (Figures 3a-b). This means that both temperature and water availability are important factors in determining future ecological conditions, and that their interactions provide a more complete, and complex, picture of changing environmental conditions. This is consistent with recent studies on climate velocity that show how spatial patterns of temperature and precipitation (Ackerly et al., 2010; Loarie et al., 2009) and evapotranspiration (Dobrowski et al., 2013) do not, and are not expected to, have identical geographic shifts over time. Therefore, future bioclimatic studies need to take into account interactions among variables when assessing potential geographic shifts in biome, ecosystem, and species ranges. However, bioclimatic studies may not capture some key factors in determining biogeography of various ecosystems. For example, the AEZ approach does include soil water availability (to incorporate soil texture) rather than simply precipitation, but not factors such as topography, daily and seasonal radiation regime, and soil type, which are also not commonly included in dynamic vegetation models (Snell et al., 2014). Furthermore, land use change has been and likely will continue to be the primary determinant of global land cover distribution (e.g., Hurtt et al., 2011; Wilkenskjeld et al., 2014), even at fine scales (Álvarez-Martínez et al., 2014).

The new AEZs also demonstrate that projected climate change makes the original land use regions bioclimatically heterogeneous over time (Figure 3c). This means that several different AEZs, and thus different environmental conditions, may exist in a single original land use region in the future, indicating that climate will not change uniformly within these regions. The original AEZs are based on 1961-1990 climate, so present day land productivity is supposedly represented by the average characteristics (i.e., yields) of these land use regions. However, we also show that these original AEZs do not provide more homogeneity of circa year-2000 crop yields within land use regions than do the

new AEZs (Figure 1). This implies that the AEZ approach does not necessarily confer a representative advantage in the present day over alternative boundary definitions, possibly due to missing factors as discussed above. Nonetheless, our results indicate that climate change would cause different rates of change in environmental conditions within different parts of each original land use region, and also changes in global AEZ area over time (Figure 3d). We obtained qualitatively similar results using the CSIRO Mk3 model outputs for generating projected AEZs for the same period (data not shown). This suggests that averaging projected climate impacts within static, climate-based land boundaries could introduce additional error into studies on land use and climate due to the mismatch of climatic assumptions.

Figure 2. Differences between new and original Agro-Ecological Zones (AEZs). Map values are changes in thematic label calculated from new minus original AEZs. Map lines delineate the 151 GCAM land use regions based on the original AEZs intersected with 14 geopolitical regions. a) Length of growing period. b) Temperature zone. c) AEZ. d) Global land area by AEZ.
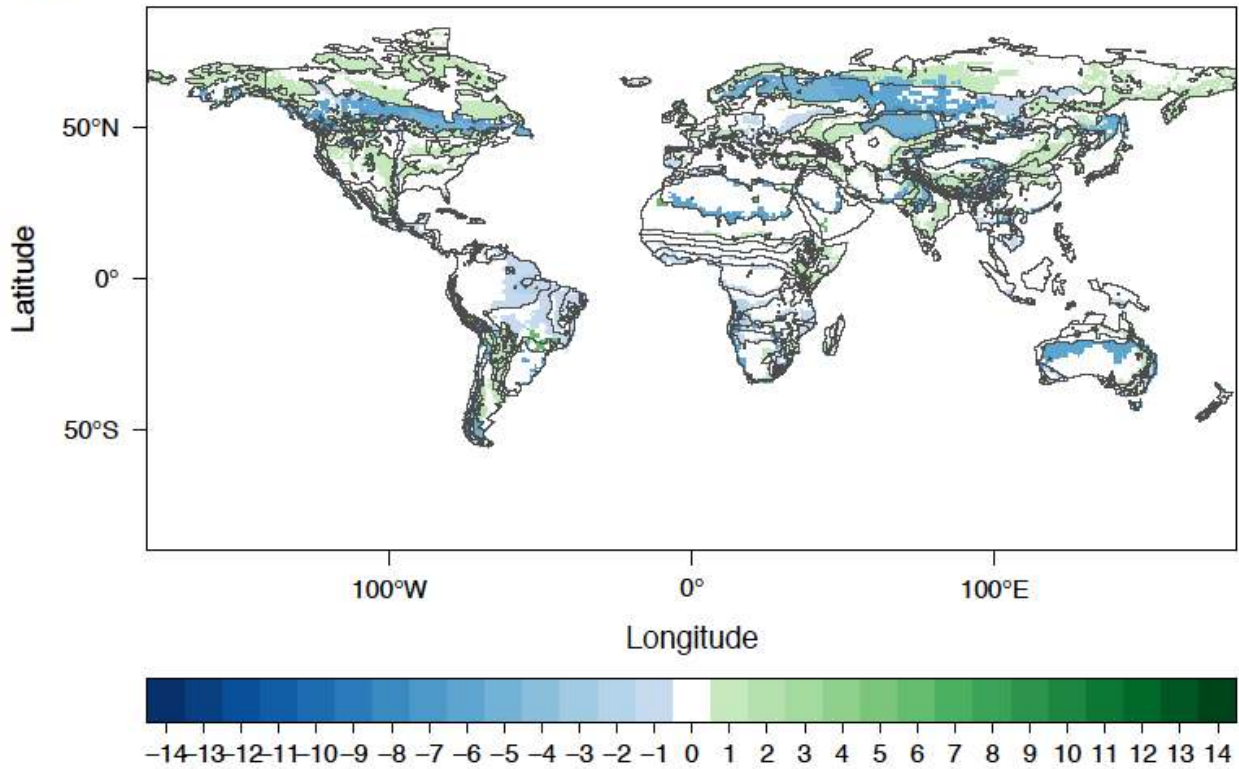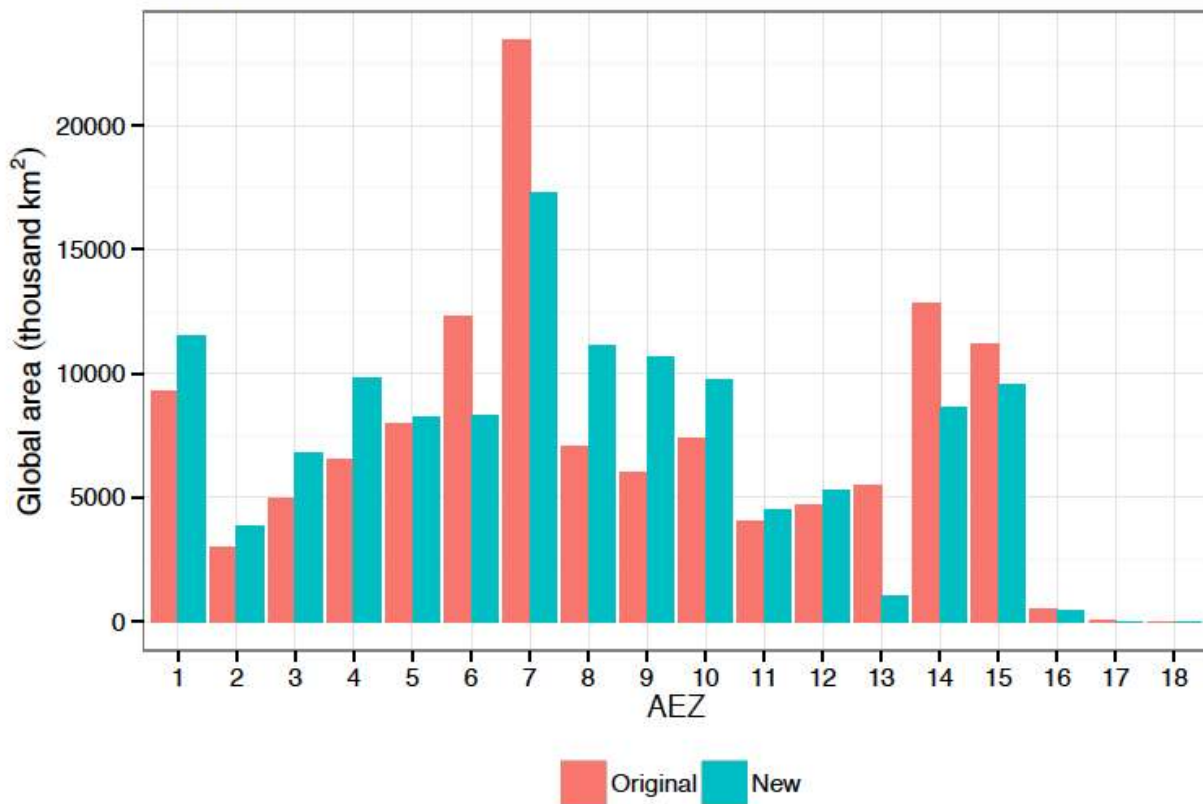
a) Difference in length of growing period bin
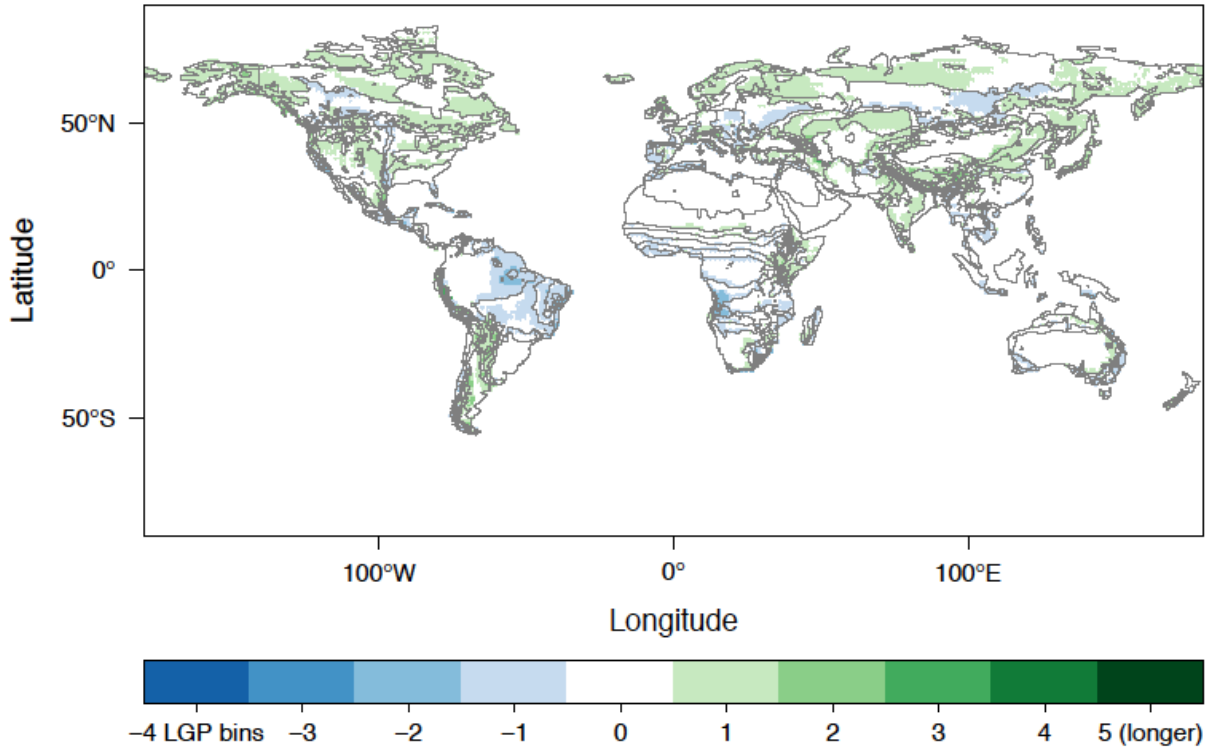
b) Difference in temperature zone

21
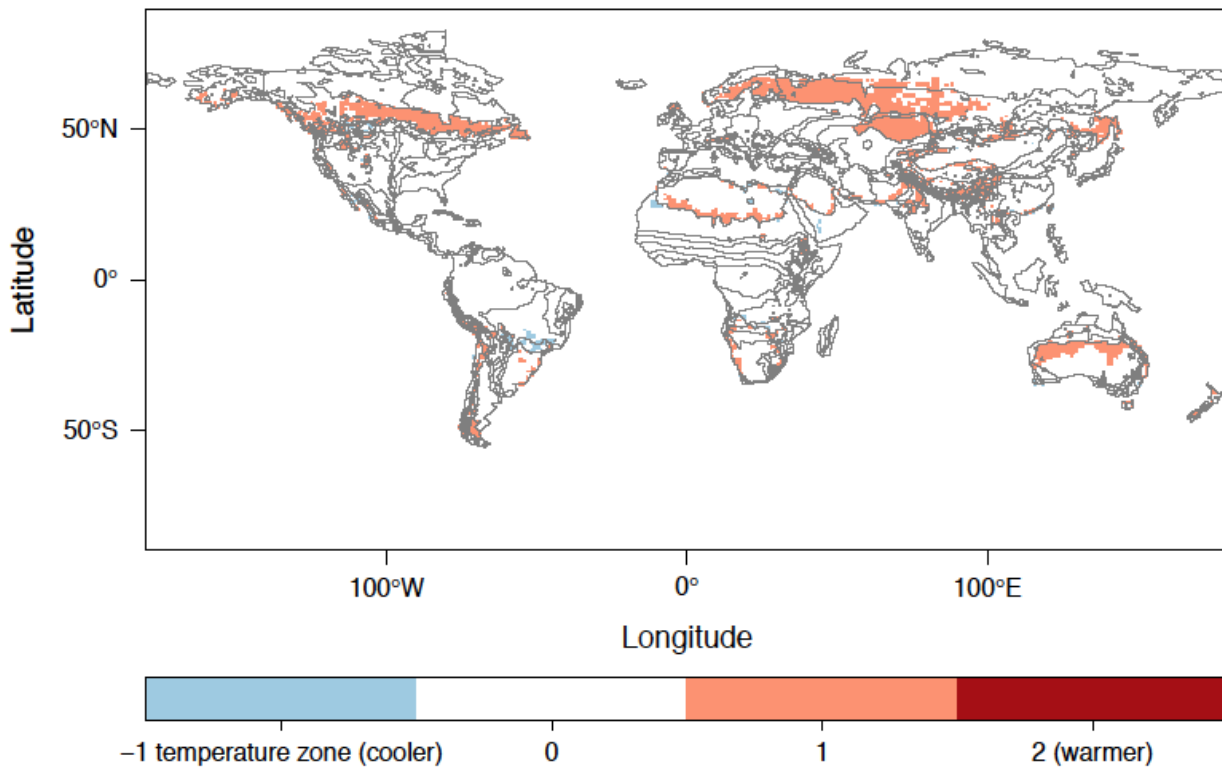
c) Difference in Agro-Ecological Zone (AEZ)
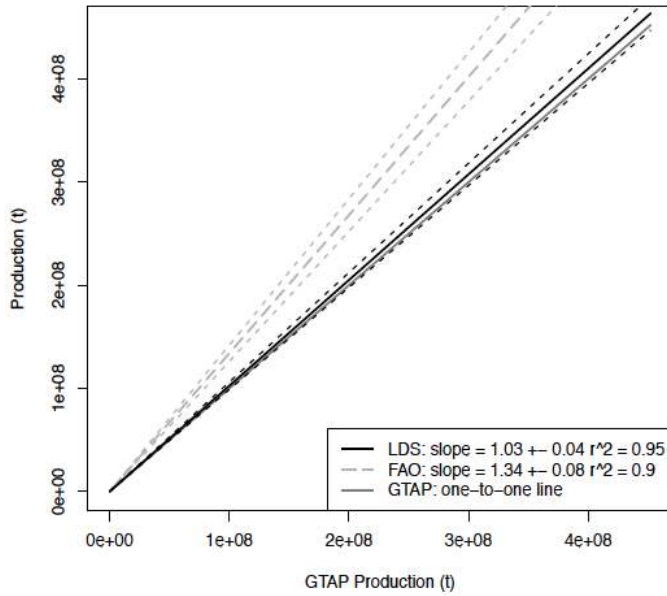

d) Comparison of global AEZ land area

3.2.   LDS evaluation against GTAP and FAO data

The LDS production and harvested area outputs for all 175 crops and the original AEZs match the GTAP data very well at the country level (e.g., Figure 4). The mean, individual crop regression slope for both production and harvested area across the 86 crops with data for at least 20 countries is 1.03 ($\pm$ 0.04 std err) with an r^2 of 0.95. Reducing the sample size to 10 for each regression includes 120 crops and gives nearly identical results. Furthermore, the LDS outputs are generally closer to FAO data than are the GTAP values, and if there is a discrepancy between the LDS and GTAP, LDS follows FAO more closely. We did not expect the larger differences between the LDS/GTAP data and the FAO data because the source gridded crop data are calibrated to the national average FAO statistics, even where sub-national level values are used (Monfreda et al., 2008; Monfreda et al., 2009). Paddy rice is a typical example of a decent match (slope = 0.92 $\pm$ 0.00 std err, r^2 = 1.00), and comparison of the cumulative distribution functions and histograms of country-level differences for production demonstrates the validity of the LDS in a less abstract manner (e.g., Figure 5). Harvested area results are effectively the same as the production results for individual crops. Nonetheless, LDS does not, and cannot, reproduce GTAP exactly, which indicates a need for increased transparency and standards for widely used data.

The primary cause of irreproducibility in these two variables is very likely the difference in the country boundaries between LDS and GTAP. An unlikely source of additional discrepancy could arise from undocumented GTAP adjustments to, or slightly different versions of, the source crop data. This additional discrepancy is unlikely because the yield and harvested area source data that we use are, to the best of our knowledge, the data developed, documented, and made publically available for use by GTAP and others (Monfreda et al., 2008; Monfreda et al., 2009). We also follow the methods exactly as documented (Lee et al., 2005; Lee et al., 2009). On the other hand, the country boundary data are different due to lack of data availability. The country boundary data used by the LDS are supposedly the source of the FAO country boundary data, but as the actual boundary data are not provided by GTAP or by FAO, it is very likely that these boundary differences are a primary source of discrepancies between the LDS outputs and both the GTAP and FAO data.

a) Production regression mean

b) Harvested area regression mean

LDS: slope = 1.03 +− 0.04 r^2 = 0.95
FAO: slope = 1.34 +− 0.08 r^2 = 0.9
GTAP: one−to−one line

LDS: slope = 1.04 +− 0.03 r^2 = 0.95
FAO: slope = 1.2 +− 0.07 r^2 = 0.9
GTAP: one−to−one line
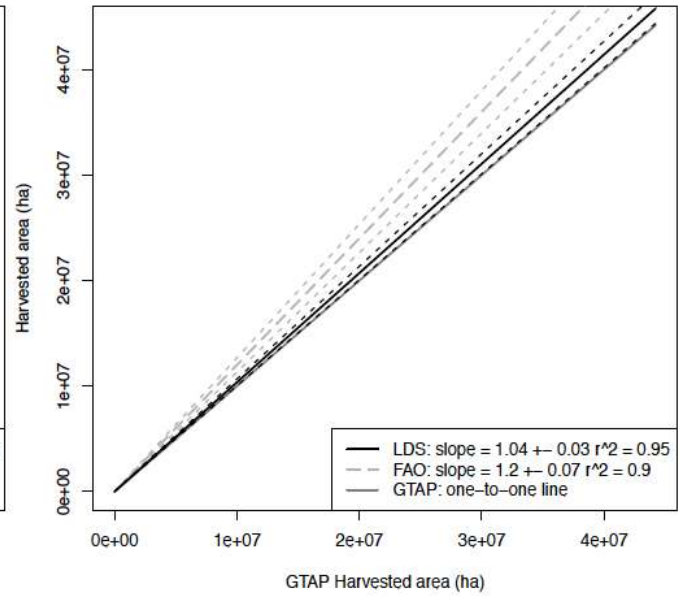
Figure 4. Country level evaluation of the Land Data System (LDS) production and harvested area. LDS outputs using the original Agro-Ecological Zone (AEZ) boundaries and the Food and Agriculture Organization (FAO) data for each individual crop are regressed against the corresponding Global Trade Analysis Project (GTAP) data. These are the mean regression values across the 86 crops with regression sample size >= 20 (i.e., present in at least 20 countries).
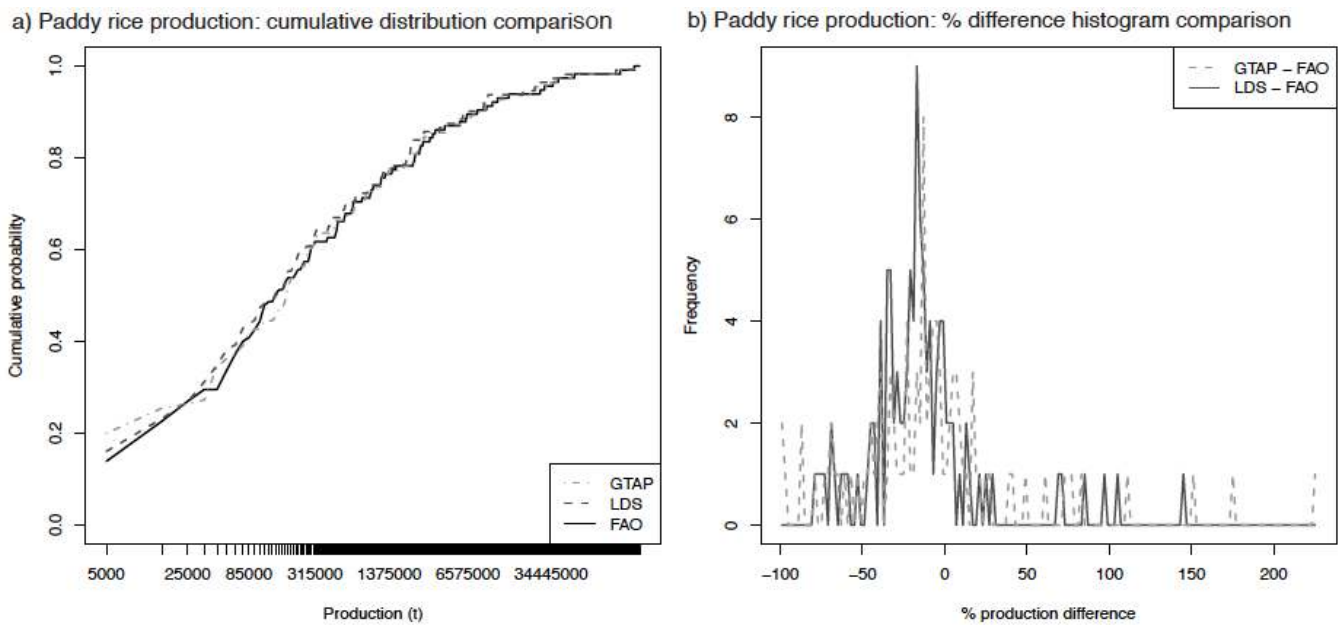
Figure 5. Individual crop example of country level evaluation of the Land Data System (LDS). These paddy rice production data represent 241 countries and the harvested area data have similar relationships among the presented data sets. a) Cumulative distribution function of rice production. b) Corresponding histograms of the LDS and Global Trade Analysis Project (GTAP) percent differences from Food and Agriculture Organization (FAO) data.

The LDS land rent outputs for the original AEZs also match well with the GTAP data at the AEZ level within GTAP regions (Figure 6). All 12 land use sectors have sufficient regression sample sizes (>= 245) to be included in the mean LDS versus GTAP regression parameters. The mean regression slope is 0.98 (± 0.01 std err), with an r^2 of 0.93, which indicates fairly high fidelity between LDS and GTAP land rents. The worst match is for the "other crops" sector, which has a slope of 0.74 (± 0.05 std err) with an r^2 of 0.36. This poor correlation is mainly due to three outliers with values greater than 3×10^9 USD (Figure 6b). Removing these outliers increases the "other crops" r^2 to 0.68 and decreases the slope to 0.70 (± 0.03 std err), which has a negligible effect on the mean regression values. Following GTAP (Lee et al., 2005; Lee et al., 2009), all land rent sector calculations except forestry use FAO price and production data in addition to the respective crop production and harvested area outputs. While some of the differences between LDS and GTAP in land rent outputs are possibly due to slightly different FAO price and production data, we have shown that the differences in crop inputs to the rent calculations are very likely due to spatial inconsistencies. Given that the average LDS accuracy for the land rent is similar to that of the production and harvested area outputs, and the land rent has the added FAO source of uncertainty, it is likely that the spatial inconsistencies between LDS and GTAP are a

25

significant portion of the land rent error. Conversely, since the additional error source did not increase the land rent error beyond that of its crop inputs, and we used the published equations for land rent (Lee et al., 2005; Lee et al., 2009), this is additional evidence to support our claim that spatial inconsistencies very likely dominate the errors in production and harvested area over any possible difference in source crop data. On the other hand, the LDS forestry land rent, which is not used by this version of GCAM, utilizes different methods and data from GTAP, yet matches the GTAP data very well (slope = 1.00 ± 1×10^{-6} std err, r^2 = 1). This good match is partially due to the fact that the LDS simply redistributes the GTAP forestry data from the original to the new AEZs, but even with such high statistical correlation the cumulative distribution function shows some deviation that arises due to this spatial redistribution (Figure 6c), which can be explained only through spatial inconsistencies between GTAP and LDS. Thus, these land rent results not only further demonstrate the irreproducibility of the GTAP data, but also support the finding that differences between LDS and GTAP are driven largely by inconsistencies in spatial boundaries arising from the lack of spatial data that directly correspond with the available tabular data. Nonetheless, LDS reproduces the GTAP land data inputs to GCAM well enough such that using either GTAP or LDS inputs generates nearly identical GCAM outputs (data not shown).

Figure 6. Evaluation of Land Data System (LDS) land rent against the Global Trade Analysis Project (GTAP) data, at the level of Agro-Ecological Zones (AEZs) intersected with GTAP regions. a) Mean of LDS versus GTAP regression values for each of the 12 sectors. b) Scatter plot of the "other crops" sector land rents, which has the worst correlation of all sectors between LDS and GTAP. c) Global cumulative distribution functions of forestry land rent.
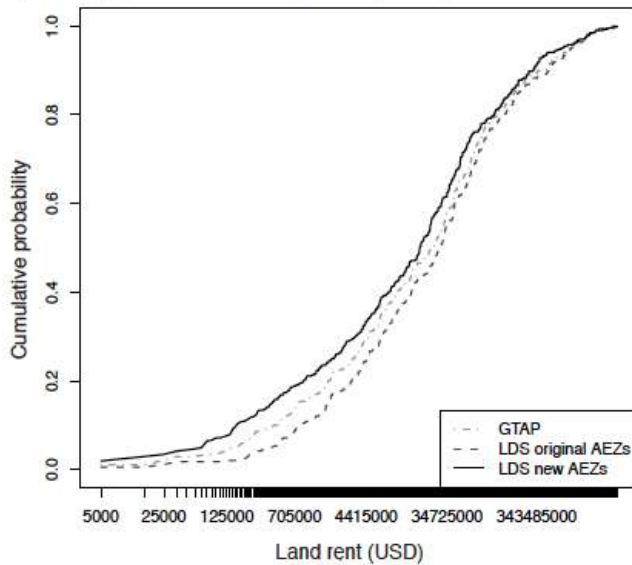
a) Land rent regression mean
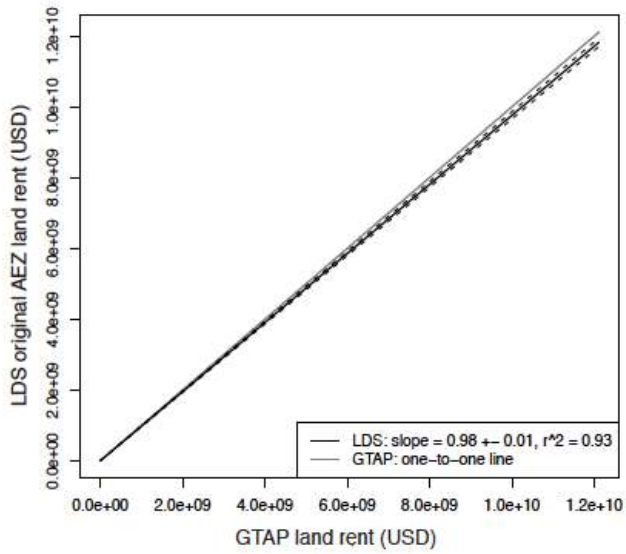
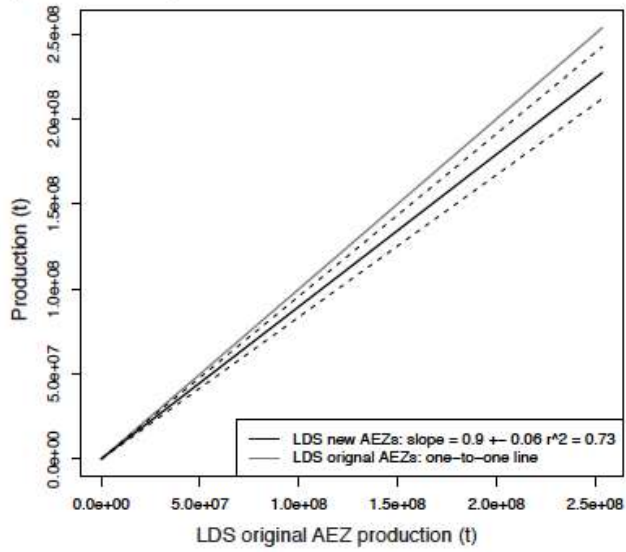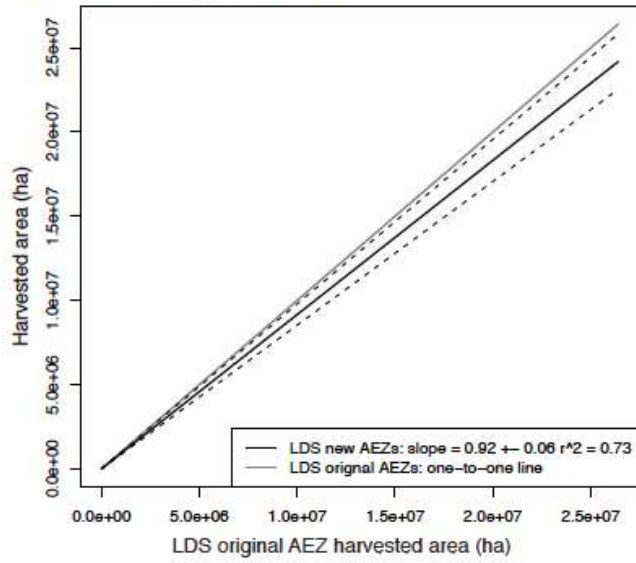
b) Direct comparison of "other crops" sector
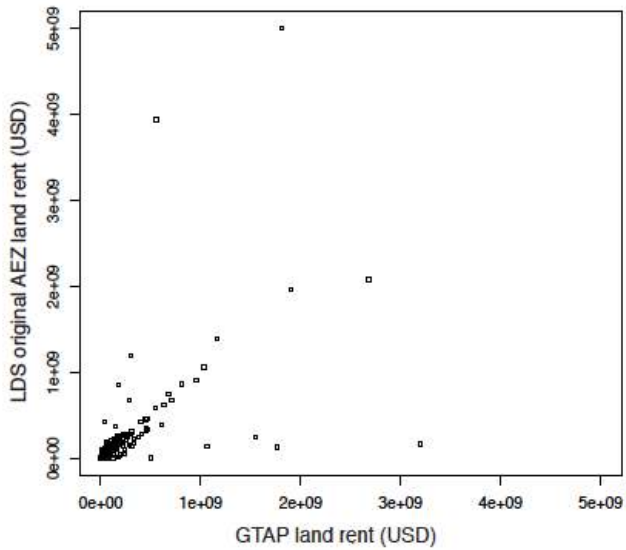
c) Forestry land rent distribution comparison

27

a) Production regression mean

b) Harvested area regression mean

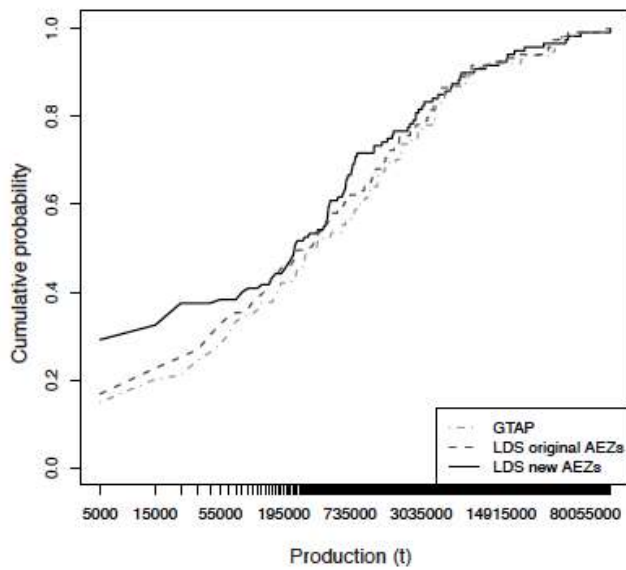## c) Paddy ride production: cumulative distribution comparison

Figure 7. Effects of new boundaries on Land Data System (LDS) production and harvested area outputs. These data are aggregated to the Global Change Assessment Model (GCAM) land use region level. a) Mean of production regressions for each of the 117 crops with sample size >= 20 (i.e., present in at least 20 countries). b) Mean of harvested area regressions for each of the 118 crops with sample size >= 20. c) Global cumulative distribution function comparison for paddy rice production.

a) Land rent regression mean

b) Paddy rice land rent: cumulative distribution comparison

- LDS new AEZs: slope = 0.91 +- 0.05, r^2 = 0.69
- LDS original AEZs: one-to-one line

- GTAP
- LDS original AEZs
- LDS new AEZs
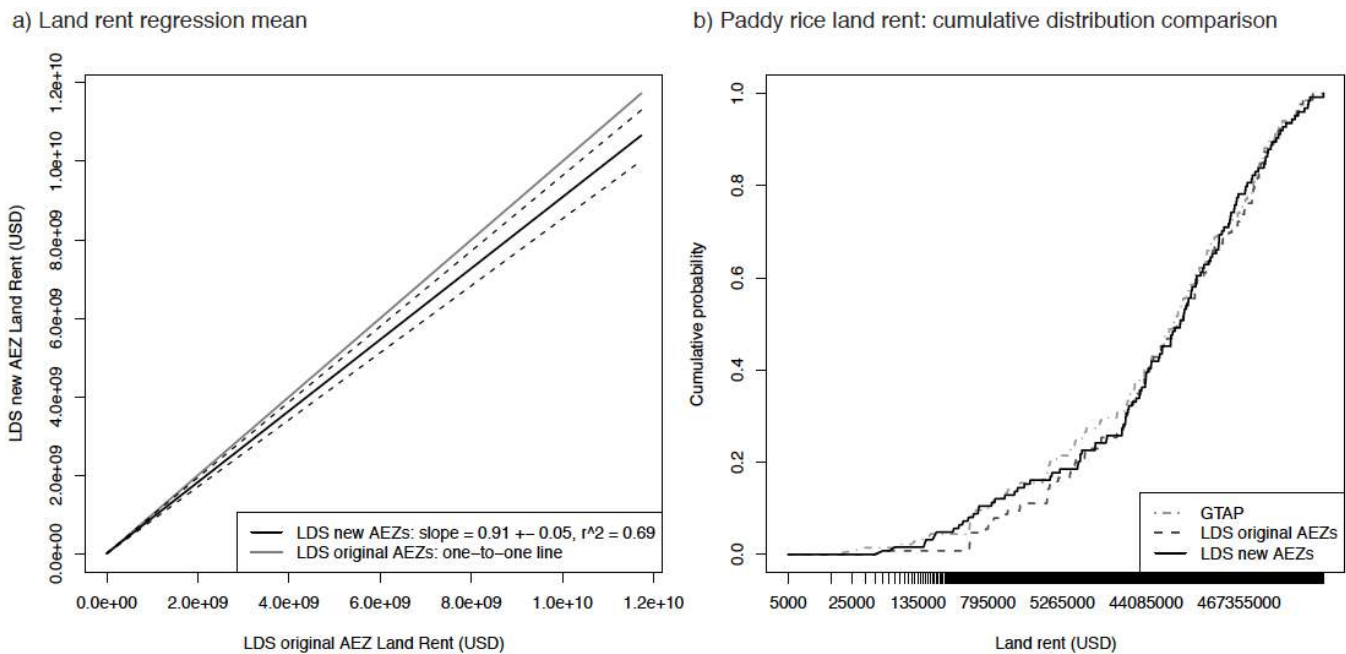
Figure 8. Effects of new boundaries on Land Data System (LDS) land rent outputs. These data are aggregated to the Global Change Assessment Model (GCAM) land use region level. a) Mean of land rent regressions for each of the 12 land use sectors. b) Global cumulative distribution function comparison for forestry land rent.

3.3. New versus reproduced original AEZ data

The differences in LDS outputs between the new and original GCAM land use regions demonstrate that using different boundaries effectively changes the simulated world. These differences generally are more pronounced for production and harvested area (Figure 7) than for the land rent inputs (Figure 8). It is important to note that the mean regression values of the new versus original outputs are not direct one-to-one comparisons because they represent only identically labeled land use regions, which are different between the new and original AEZ boundary sets. For example, there are 151 land

use regions in the original set and 184 land use regions in the new set. They are still instructive, however, in that they clearly demonstrate the differences in initial conditions where the same AEZs exist in any land use region for both AEZ boundary sets. Crops are included in the mean values only if they exist in at least 20 countries. The mean slopes for crop production (117 crops) and harvested area (118 crops) are 0.90 (± 0.06 std err) and 0.92 (± 0.06 std err), respectively, each with an r^2 of 0.73. These slopes are clearly different than one, indicating that the new land use regions give a distinctly different representation of the world than the original land use regions. The cumulative distribution function of paddy rice presents a good example of how the global distribution of values changes due to the new land use regions (Figure 7c). Each crop does respond uniquely to the new boundaries, however, which has important implications for GCAM land resource projection because land use area shares are determined by the relative profitability of each land use within a land use region.

Likewise, the global distributions of land rent also shift with the new land use regions, separating the new simulated world farther from the original one (Figure 8). All 12 land use sectors are included in the mean regression values, and as for the crop data, these regressions are made between the identically defined AEZs, which cover different areas in the two land use region sets. The mean slope is 0.91 (± 0.05 std err, with $r^2 = 0.69$), which is also clearly different than one. The sensitivity of these initial land data to spatial aggregation also becomes apparent when comparing the forestry land rent cumulative distribution functions for the GCAM land use regions (Figure 8b) with those for the AEZs within GTAP regions (Figure 6b). While there is an obvious shift in the global distribution at the native GTAP resolution (AEZs intersected with 87 regions), aggregating to the GCAM land use regions (AEZs intersected with 14 regions) reduces this shift. The regression values correspond with the global distributions, with the slope for GCAM regions (0.96 ± 0.05, $r^2 = 0.74$) being closer to one than the slope for GTAP regions (0.90 ± 0.03, $r^2 = 0.71$). Overall, spatial boundaries are a primary determinant of the how the world is represented, which directly impacts global simulations, and ultimately affects how we understand global change.

3.4.   GCAM simulations

GCAM's land resource projections vary between the original and new AEZ simulations, indicating that simply changing the boundaries of the initial land data drives the whole system in a different direction. More specifically, different boundaries drive dramatic differences in land use and cover, associated emissions, crop production and price, and bioenergy production and consumption.

The mechanics responsible for divergent model outcomes are reviewed briefly here. In each GCAM land use region, land is allocated among up to 20 competing uses according to the relative

profitability of each land use. Because this allocation is done on the basis of shares, modifying the size of a land unit will result in different land quantities, all else equal. However, changing the land use region boundary also changes base-year productivity and therefore profitability of each land use in each land use region, which can lead to divergent land shares over time. Furthermore, dedicated bioenergy crops do not have base-year data; instead, their future shares depend on their profitability in relation to that of the dominant crop in the base-year in each land use region. By changing the characteristics of the base-year crop production in each land use region—harvested area, production, and yield—the comparative future profitability of bioenergy in each region may also be affected.

Fodder crops, bioenergy crops, and intensive pasture have substantial percent differences in global area by 2100 between the new and original AEZ simulations, with grain crops also having a distinct difference (Figure 9a and Table 4). These differences are more pronounced when considered as percentages of the original projected change from 2010 to 2100. In particular, total grain crop area is only 3.5% less with new AEZs, but this difference is a 67% decrease in the originally projected increase. As Figure 2d shows, the new AEZs generally have more land in relatively productive AEZs, and less land assigned to relatively unproductive AEZs, specifically 7, 13, 14, and 15. The enlarged AEZs overlap somewhat with their original counterparts, increasing agricultural expansion via the mechanisms described above. The increase in total end-of-century cropland area with new AEZs is 204,000 km^2 (1.4% of original AEZ value), which is 7.7% of the range covered by RCPs 2.6, 6, and 8.5 in 2100 (van Vuuren et al., 2011a). Differences at the regional level can be even greater (e.g., Figure 9b and Table 4) than global differences, and often include substantial differences in other crops and harvested forest. This is because the regional differences will reflect spatial tradeoffs in land use region expansion and contraction combined with regional changes in relative productivity among crops. The net change in global area for any given land type is the net result of these spatially driven regional tradeoffs.

While the effects of new boundaries on area can be considerable for particular crop groups, both globally and regionally, the relative sizes of these effects vary when aggregated to all cropland and compared with an AgMIP study that uses ten global agro-economic models to estimate changes in cropland area from 2005 to 2050 (Schmitz et al., 2014). Globally, the AgMIP study reports a range of cropland expansion from about 1% to 26% for a baseline scenario with SSP2 population and GDP, without climate change impacts (for the seven models that include bioenergy crops), with GCAM having an 11% increase. Our study shows that using the new AEZ boundaries increases cropland expansion from 13% to 14% over the same time period. For the former Soviet Union, however, our study shows an increase from 7.1% to 10% for cropland expansion due to the new AEZ boundaries, while the AgMIP reports a range of ±23% for cropland area change, with GCAM having the maximum

expansion. Note that the differences in GCAM's output between these two studies reflect different assumptions about population, GDP, and future yield growth, all of which were harmonized among the AgMIP models to values that differ from GCAM's native and modified assumptions used in this study. Regardless of these differences, the main point of this comparison is that the difference in projected global cropland expansion by 2050 due to the new AEZ boundaries is 6.2% (123,938 km^2) of our original expansion estimate, 6.5% of their model-average expansion estimate without climate impacts, and 10% of their model-average expansion estimate attributed solely to projected climate impacts. Even though we do not address climate impacts in this study, this comparison demonstrates that different boundaries can potentially have a substantial influence on projected changes in global cropland area when climate impacts are included.
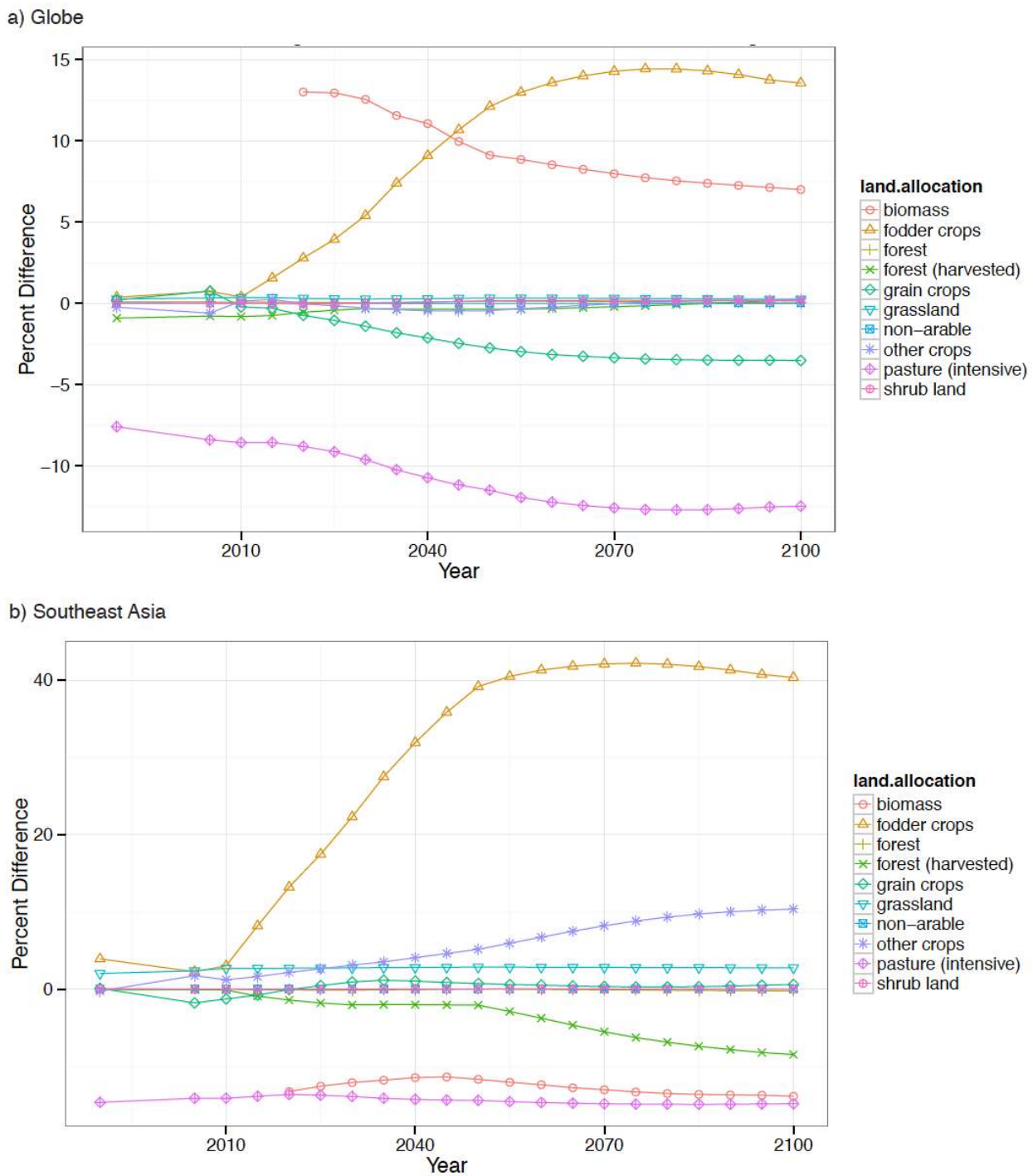
a) Globe

b) Southeast Asia

Figure 9. Percent difference in projected land use and cover area (new – original AEZs).

Table 4. Projected land use and cover area in year 2100 (thousand km^2).

Land type	Global				Southeast Asia			
	Original AEZs	Difference: new – original AEZs	Difference as percent of original	Difference as magnitude percent of 2010 to 2100 change in original	Original AEZs	Difference: new – original AEZs	Difference as percent of original	Difference as magnitude percent of 2010 to 2100 change in original
Biomass	3869	271	7.0	7.0	278	-39	-14	14
Fodder crops	1061	144	14	43	10	4	40	63
Forest	35758	4.4	0.01	0.2	2409	-6	-0.2	2.8
Harvested forest	4442	9.2	0.2	0.7	172	-15	-8.5	41
Grain crops	6425	-226	-3.5	67	598	4	0.6	9.1
Grassland	40082	97	0.2	4.0	628	17	2.8	29
Non-arable	19447	0	0.0	0.0	430	0	0.0	0.0
Other crops	6254	16	1.8	0.3	640	66	10	800
Intensive pasture	2664	-333	-12	38	218	-32	-15	37
Shrubland	6933	9.8	0.1	2.8	385	-0.05	-0.01	0.2

Differences in area translate directly into dramatic differences in regional and global crop production. Global crop production shifts toward more palm fruit, fodder crops (grasses and herbaceous), and away from intensive pasture and bioenergy crops by 2100 (Figure 10a, Table 5). As with area, regional shifts in production due to the new land use regions drive the global changes, and these changes are a large portion of the original projected change from 2010 to 2100 for several crops. The increase in palm fruit (oil palm) production with new AEZs is particularly interesting, as it highlights a large sensitivity in model output to initial conditions and land use region size that may be mitigated somewhat by applying climate impacts to crop yield. With new AEZs defined by future climate, about 9% of total, base-year oil palm production is shifted from AEZ 6 to the drier and larger AEZs 4 and 5. Because oil palm prices increase in both scenarios due to demands from the energy system, and yields are not modified to reflect climate change, the profitability of the oil palm increases over time, as do the shares of land allocated to oil palm production. However, the new AEZ scenario with more base-year oil palm production in AEZs 4 and 5 sees more expansion in total land area and production primarily because the land use regions in which is it produced have increased in size.

Differences in crop prices are consistent with differences in area and production, with intensive pasture and fodder experiencing the most dramatic price changes (Figure 10b, Table 5). Note that the global supply/demand equilibria associated with these prices depend for each crop on the price elasticities of the various demands (food, animal feed, bioenergy, and other uses). Crops that are used mostly for food (e.g., wheat, sugar, rice) tend to have low assumed price elasticity or substitutability, and thus smaller supply/demand changes with new AEZs. In contrast, crops used mostly or exclusively for bioenergy or fodder tend to be relatively price-elastic and have larger changes in response to new land use regions. These crops are readily substitutable in the energy transformation and meat production sectors, respectively, and the quantities of the final commodities (e.g., refined fuels, meat) demanded by consumers are also price-responsive.

Table 5. Global crop production and prices in year 2100.

Land type	Production (Mt)				Prices (1975$/t)			
	Original AEZs	Difference: new – original AEZs	Difference as percent of original	Difference as magnitude percent of 2010 to 2100 change in original	Original AEZs	Difference: new – original AEZs	Difference as percent of original	Difference as magnitude percent of 2010 to 2100 change in original
Biomass	5898	-434	-7.4	7.4	26.45	0.37	1.4	10
Corn	1383	-19	-1.4	3.5	35.11	-0.40	-1.1	11
Fiber crop	101	-2.3	-2.3	8.2	169.84	-1.03	-0.61	10
Fodder grass	1216	150	12	36	41.58	-9.24	-22	58
Fodder herb	1756	168	9.6	20	51.18	-8.64	-17	60
Forest (harvested)	2289	0.0	0.0	0.0	114.08	0.35	0.3	1.2
Miscellaneous crop	2164	-5.5	-0.3	1.3	185.11	1.92	1.0	45
Oil crop	604	-19	-3.1	9.9	68.88	-0.83	-1.2	13
Other grain	417	-7.9	-1.9	6.5	35.71	-0.38	-1.1	16
Palm fruit	1093	256	23	32	28.28	-1.78	-6.3	26
Pasture (intensive)	3073	-134	-4.4	14	44.26	-4.53	-10	24
Rice	954	-6.7	-0.7	2.3	51.38	0.66	1.3	24
Root tuber	1125	-0.2	-0.02	0.06	55.61	-2.10	-3.8	60
Sugar crop	2981	-46	-1.5	4.5	12.39	0.12	1.0	18
Wheat	860	-5.1	-0.6	2.9	26.45	0.37	1.4	27

Table 6. Biomass energy production in year 2100.

Region	Biomass energy (EJ)		
	Original AEZs	Difference: new – original AEZs	Difference as percent of original
Global	109	-8.0	-7.4
Latin America	12	-0.04	-0.3
Africa	12	2.5	21
Australia and New Zealand	2.8	-1.3	-48
Canada	2.8	-0.3	-11
China	11	-2.0	-19
Eastern Europe	14	-5.6	-39
Former Soviet Union	14	-0.3	-1.9
India	6.3	4.2	66
Japan	1.0	-0.4	-35
Korea	0.2	-0.1	-45
Middle East	3.1	-0.2	-7.8
Southeast Asia	8.1	-2.1	-26
USA	12	-2.0	-17
Western Europe	11	-0.3	-3.0

Dedicated crops for biomass energy are first available in 2020 in these simulations, and the global reduction in crop biomass energy production with new AEZs (Figure 10c, Table 6) despite an increase in bioenergy crop area (Figure 9a, Table 4) is due to lower average yields globally and within each geopolitical region. The new AEZ boundaries aggregate lower-yield areas with higher-yield areas in such a way that lowers average yields in land use regions that are important for bioenergy crop production. As these lower values are part of the initialization data, biomass crops need more area to produce less energy in 2020, and this relationship persists through 2100. The global, dedicated-biomass, primary energy production of 63 EJ in 2050 with original AEZs is within the range of recently revised estimates of maximum production ranging from 45-111 EJ (Searle and Malins, 2015). The 4.6 EJ (7.3%) decrease in 2050 with new AEZs is 7% of this range of maximum potential production, which is high

considering that the GCAM estimates are market-based rather than maximized, but is well within the range of future biomass energy projections in GCAM and in IAMs in general (Fischedick et al., 2011). The regional sensitivity of biomass energy production to land use region boundaries is much greater than the global sensitivity, with India being exceptionally sensitive due to the doubling in size of AEZs 4 and 10 and the change in relative crop productivity in AEZs 2 and 3, both of which lead to increases in biomass crop area. The differences in land resource projections due to new AEZs do influence energy markets enough to change the amount of electricity produced by biomass (-2%, or -86 TWh, by 2100) and the total amount of biomass bioenergy consumed across all sectors (-2.7%, or -4.6 EJ, by 2100). These results demonstrate that the integrated energy-land system is fairly sensitive to the spatial delineation of the earth.

Figure 10. Percent differences in a) global crop production, b) biomass energy production, and c) global crop prices (new – original AEZs).
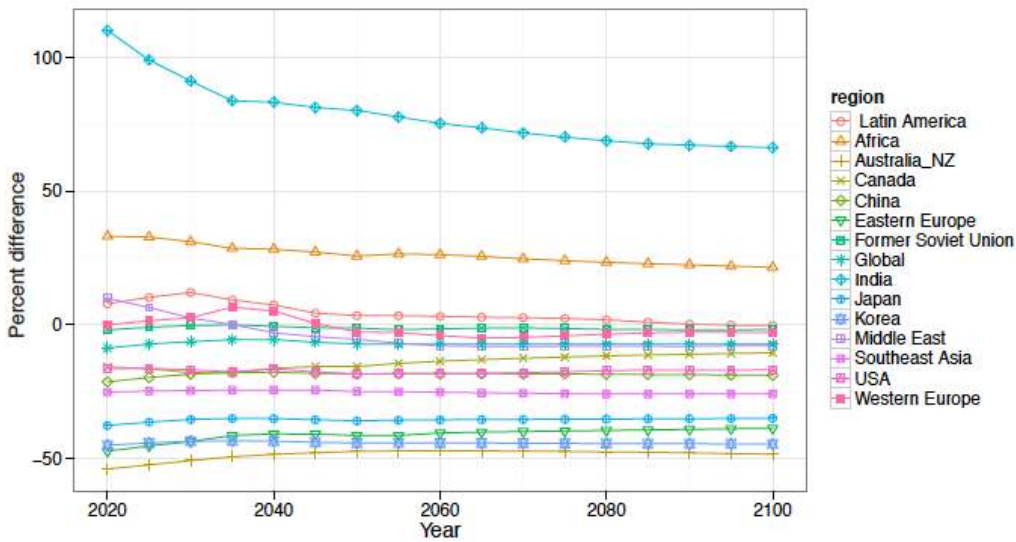
a) Global crop production comparison
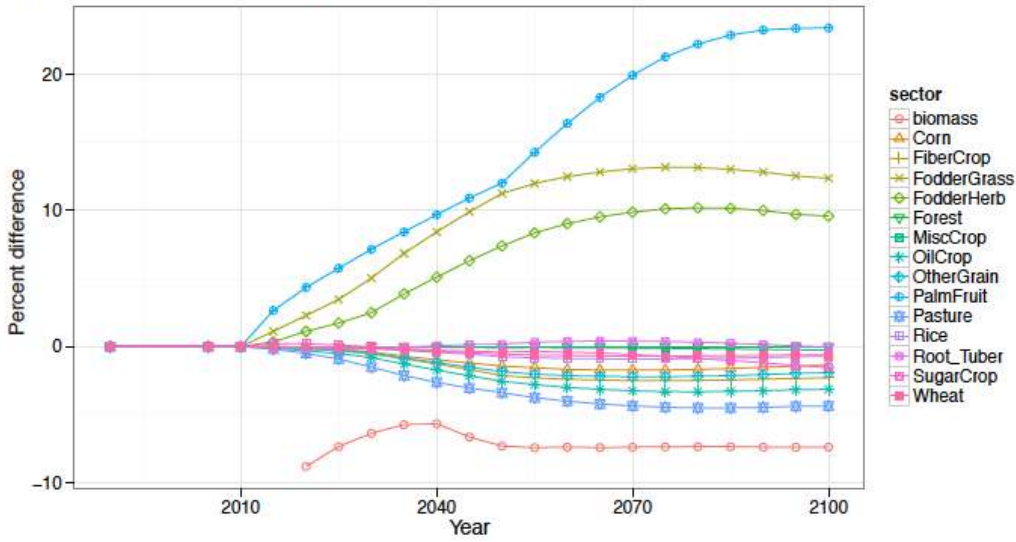
b) Global crop price comparison
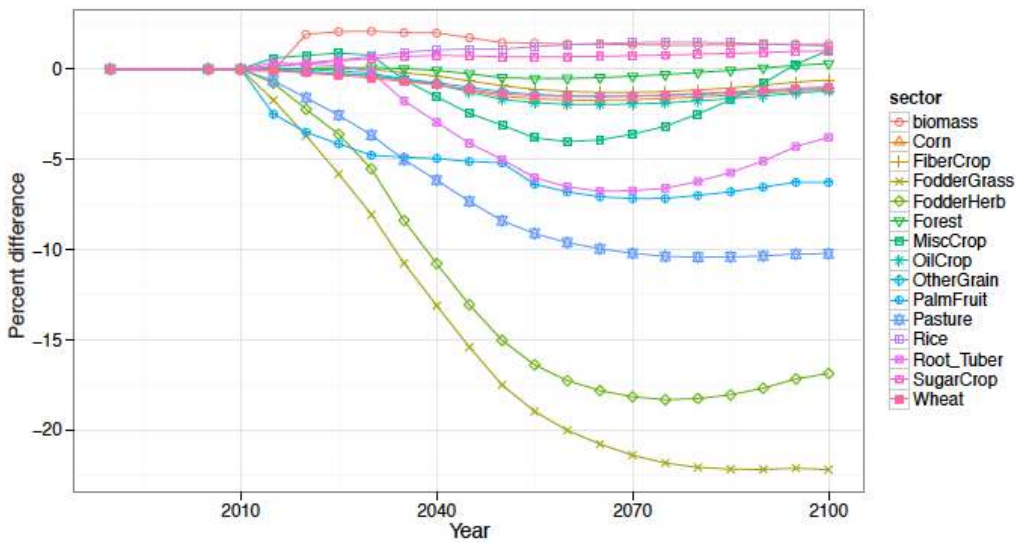
c) Global biomass energy production comparison

The differences in land use and cover between the simulations also drive differences in net annual land use and cover change CO_2 emissions at both the regional and global levels (Table 7). Note that divergent global land use change emissions are observed even in the historical period. This results from GCAM's method of calculating land use change emissions, which is based on net changes in different land use types over time within individual land use regions. Grid cells are aggregated to regions prior to performing the emissions calculation, and aggregating grid cells differently can change the extent of historically offsetting land use changes within land use regions.

From the first projection year (2015) forward the globe is a net sink for land use change emissions largely due to land use changes during the historical period that favor forest regrowth and discourage crop expansion after 2010. From 2020 to 2050, the annual strength of this sink increases with the new AEZ boundaries by as much as 40 Mt C per year, but after 2055 this increase declines to zero by 2100. At the regional level, the relative differences in net emissions can be very large while the absolute values remain comparable to the global values. Despite the complexity of accounting and tracking land use change emissions, it is crucial to reduce this uncertainty associated with land use region boundaries because land use and cover change emissions currently contribute significantly to anthropogenic radiative forcing (11% of total CO_2 emissions for 2002-2011; Le Quere et al., 2013), and could become an even greater share of total emissions under climate target scenarios that reduce the amount of fossil fuel emissions by the end of the 21st century, such as RCPs 2.6 and 4.5 (van Vuuren et al., 2011a).

Table 5. Projected global land use and cover change CO_2 emissions (MtC yr^{-1}).

Year	original AEZs	new – original AEZs[a]
1980	977	14
1985	1026	14
1990	1016	14
1995	756	10
2000	703	-2
2005	625	-9
2010	712	-40
2015	-720	34
2020	-553	-16
2025	-477	-4
2030	-290	-5
2035	-99	-20
2040	-78	-14
2045	-27	-26
2050	-5	-24
2055	2	-15
2060	-58	-7
2065	-84	-6
2070	-78	-4
2075	-82	-5
2080	-83	-6
2085	-78	-5
2090	-69	-5
2095	-65	-3
2100	-60	0

[a]Negative difference indicates less emissions or a larger sink with new AEZs.

3.5. Implications for modeling land change under climate change

Given the spatial heterogeneity of environmental factors and potential climate impacts (section 3.1) and the uncertainty introduced by land use region averages (section 3.4), the application of climate impacts, as aggregated to land use regions from gridded model output, will likely decrease the

homogeneity of land productivity, which is a key reason for the use of AEZs in land use modeling. In turn, this seems likely to increase associated model uncertainty in land resource projections. That said, it is unclear even if AEZs as currently implemented actually provide sufficient homogeneity (Figure 1) for the modeling assumption of representative averages to hold for model initialization, regardless of whether or not climate impacts are incorporated. For example, native GCAM spatially assigns biomass crop characteristics and ecosystem carbon densities by AEZ (section 2.1). Spatial uncertainty is introduced if the homogeneity and/or location of these AEZs do not actually coincide with GCAMs assumptions about relationships between AEZs and land characteristics. Additionally, such assumptions that rely on static AEZ boundaries preclude consistent implementation of climate impacts because the boundaries and assumptions would remain the same while productivity changes heterogeneously over time within these boundaries. Even if the boundaries and assumptions were not tied to AEZs, averaging across this increasing heterogeneity and applying the results as representative values for each land use region would introduce additional uncertainty to model projections. This additional uncertainty is directly related to the boundaries themselves, thus it is important to first characterize uncertainty due to land use region boundaries without the additional effects of potential climate impacts.

Quantifying the effects of spatial uncertainty on land resource projection is also important for scenario based climate modeling in general, which does not yet incorporate feedbacks from climate to land modeling. The CMIP process separates climate impacts from scenario generation, and as such the scenarios contain spatial uncertainty, free from the effects of climate, that can influence impact studies. For example, Brovkin et al. (2013) show that projected land use change significantly affects local to regional climate, but unfortunately the six ESMs evaluated did not agree on the magnitude, sign, or location of these climate effects. They concluded that the differences among the model outputs were due mainly to differences in land use and cover change implementations and corresponding spatial distributions of land cover. These distributions, however, included uncharacterized uncertainty associated with the spatial land surface delineation of the driving IAM. A different set of spatial boundaries in the IAM would generate a different land use projection that would then be uniquely implemented in each ESM, giving a different set of results due to the direct biophysical effects of land use and cover change (e.g., Jones et al., 2013). Thus, it is critical to characterize and reduce the uncertainties associated with the spatial delineation of the earth surface in both IAMs and ESMs in order to adequately project climate change.

Gridded climate projections are input to various impact models, and several recent and ongoing assessments have aggregated grid- or farm-scale crop model output to larger scales in order to allow climate impact assessments using models of different scales (e.g., von Lampe et al. 2014; Beach et al.

2015). For the AgMIP inter-model comparison, Müller and Robertson (2014) aggregated half-degree crop model output, which was driven by ESM climate projections, into 115 country and multi-country regions, using base-year harvested area as the weighting factor, allowing an average climate-related change in yield for each crop to be computed for each of these regions. Thus, the assumption in the AgMIP studies is somewhat analogous to that of the AEZ approach in IAMs—i.e., that agricultural productivity may be approximated for entire land use regions via weighted aggregation of potentially heterogeneous grid cells—but differs in that the defining criteria for the land use regions are political, not climatic. As such, the criteria for defining land use regions are not affected by climate change. This example not only demonstrates how the IAM and ESM spatial uncertainty is propagated through scenario based climate projection to impact analysis, but also shows how land region delineation would contribute to uncertainty when averaging climate impact feedbacks into IAM land projection.

Increasingly, studies are including climate change impacts on land projection to incorporate these feedbacks, and as these feedbacks are implemented the potential for increasing error due to spatial mismatch also increases. Studies modeling climate change impacts in GCAM (e.g., Calvin et al., 2013; Di Vittorio et al., 2014; Kyle et al., 2014) apply average changes to crop productivity in the AEZ-based land use regions, even though the changes may not be consistent with the boundaries, mainly because the spatial structure of the model is fixed. Two other feedback studies also assume that climate impact averages are representative over time, even though they use only 16 geopolitical regions for land use projection (Kicklighter et al., 2014, Reilly et al., 2012). While the geopolitical regions are not climatically determined, they are quite large and so the averages may not be representative, which is why several IAMs have disaggregated their geopolitical regions and in some cases introducing new issues related to climatic delineation. Our results suggest that spatial land boundaries in land use models should not be determined by climatic factors that may change, but rather by physical (e.g., watershed) or imposed (e.g., grid) factors that are unlikely to change over the simulated time period. While these alternative boundary definitions will not eliminate the sources of spatial uncertainty identified above, they have the advantage that they can be more easily constructed and do not lose their defining criteria over time, because they are not tied to climate.

4. Conclusions

The two main purposes of this study are 1) to evaluate the utility of climatically-defined boundaries, AEZs in particular, for long-term agricultural sector projections in the context of a changing climate, and 2) to quantify the sensitivity of GCAM land resource projections to land use region boundaries, without applying climate impacts. Using AEZ boundaries defined by a future climate

realization reveals inconsistencies in agro-economic modeling assumptions when considering future climate change, and also leads to a very different trajectory of land use distribution in GCAM at regional and global levels, with dramatically different land resource projections through 2100. The main implications for land change modeling are that 1) greater care must be taken when delineating land use regions and 2) the uncertainty associated with this delineation must be quantified.

Importantly, climate-induced shifts will cause historical-climate-based land use regions to become heterogeneous over time with respect to climate impacts on land productivity. This heterogeneity violates the modeling assumption that the average vegetation productivity adequately describes the area for purposes of land resource projection over the upcoming century. The effects of this misrepresentation may be relatively small in this study compared to the effects of changes in the initial state of the world because here the homogeneity assumption applies mainly to prescribed rates of forest growth and technological yield improvement, and also because the historical and projected AEZs provide nearly identical levels of homogeneity in the initial crop yields. However, when including climate impacts on crops and vegetation, averaging productivity over increasingly heterogeneous land units will likely introduce substantial error into land resources projections. Note that in this study, we have not applied any changes to the land productivity consistent with future climate impacts; for this reason, the results with new AEZs should not be seen as representative of agriculture under a changing climate. This point is particularly illustrated by the results for future oil palm production, where the future production is actually increased by shifting a portion of total, base-year production from historical AEZ 6 to future, drier, and enlarged AEZs 4 and 5, a shift which indicates a likely, climate-induced reduction in productivity over time for this crop (an effect not considered in this study). Instead, the results should be interpreted to indicate the importance of base-year AEZ initialization for future long-term agricultural and energy system projections. The demonstrated importance of the initial model state and its dependence on land use region boundaries suggests that climate-based delineations of land use regions and their associated assumptions may not be appropriate for studies involving climate change. While any set of static boundaries will have uncertainties associated with it, we suggest defining boundaries using factors that remain fixed over time, so as to eliminate additional uncertainties associated with dynamic boundaries and reduce the potential for a false sense of homogeneity at any given point in a simulation.

Resulting differences in land use and cover change and bioenergy production affect net land use change CO_2 emissions and the mix of energy production, respectively, demonstrating that GCAM's whole energy-land system shifts in response to a different spatial delineation of the earth surface. Year 2100 differences in global area of biomass energy crops (+7%), fodder grass (+14%), and intensive

pasture (-12%) are quite large with new AEZs, and regional differences can be even larger. These area differences correspond with changes in crop yields, production, and prices, which propagate through to the energy system, where biomass demands by the electricity and refining sectors are lower. The observed differences are generally explained by the land sharing algorithms in GCAM—wherein total land cover by land use type is affected by the size of the land use regions—and by the sensitivity to base-year-calibrated, within-region land allocations and yields, which are also affected by the shape and position of the land units.

We have been able to achieve these results by implementing a land data system that generates reproducible data for an arbitrary set of AEZ boundaries from publically available data sets. This system effectively reproduces the original GTAP land data used by GCAM, but not exactly due to lack of available spatial data that corresponds directly with the tabular data. Nonetheless, GCAM simulations using GTAP or the original AEZ LDS outputs generate nearly identical results. Furthermore, individual crop production and harvested area outputs from LDS generally match FAO data better than the GTAP data at the country level. The LDS has increased value over a single data set in that it enables flexible disaggregation of geopolitical boundaries, based on application-specific criteria, such as the desire to optimize land use regions to minimize error introduced by heterogeneity of climate impacts to agriculture and ecosystems over time. It also offers a self-consistent method for transforming gridded, initial-state land data to a variety of model-specific spatial structures, which could be useful for multi-model studies.

Software Availability

The Land Data System (LDS) is C code, with additional support scripts written in R. The source code is less than 1 MB, the executable is about 200 kB, and the included input data is about 12 GB. The user must also download about 37 GB of additional input data. The LDS requires Linux or Mac OS X (Xcode is useful, but not necessary), the R statistical software (https://www.r-project.org), the NetCDF library, and 2 GB of RAM. The code has been written in standard C, so it should also compile on Microsoft Windows/DOS, with the appropriate tools, although this has not been tested. Alan Di Vittorio developed this code at Lawrence Berkeley National Laboratory, and it is available from the developer at no cost for non-commercial use only. Contact information:

Alan Di Vittorio

Lawrence Berkeley National Laboratory

Climate and Ecosystem Sciences Division

One Cyclotron Road, MS 74R316C

Berkeley, CA 94720-8268

510-486-7798

avdivittorio@lbl.gov

References

Ackerly, D.D., Loarie, S.R., Cornwell, W.K., Weiss, S.B., Hamilton, H., Branciforte, R., Kraft, N.J.B., 2010. The geography of climate change: implications for conservation biogeography. Diversity and Distributions 16(3) 476-487.

Adam, J.C., Lettenmaier, D.P., 2003. Adjustment of global gridded precipitation for systematic bias. J. Geophys. Res. 108(D9) 4257.

Álvarez-Martínez, J.M., Suárez-Seoane, S., Stoorvogel, J.J., de Luis Calabuig, E., 2014. Influence of land use and climate on recent forest expansion: a case study in the Eurosiberian–Mediterranean limit of north-west Spain. Journal of Ecology 102(4) 905-919.

Beach, R.H., Cai, Y., Thomson, A., Zhang, X., Jones, R., McCarl, B.A., Crimmins, A., J. Martinish, Cole, J., Ohrel, S., DeAngelo, B., McFarland, J., Strzepek, K., Boehlert, B., 2015. Climate change impacts on US agriculture and forestry: benefits of global climate stabilization. Environmental Research Letters 10, 095004.

Brovkin, V., Boysen, L., Arora, V.K., Boisier, J.P., Cadule, P., Chini, L., Claussen, M., Friedlingstein, P., Gayler, V., van den Hurk, B.J.J.M., Hurtt, G.C., Jones, C.D., Kato, E., de Noblet-Ducoudre, N., Pacifico, F., Pongratz, J., Weiss, M., 2013. Effect of Anthropogenic Land-Use and Land-Cover Changes on Climate and Land Carbon Storage in CMIP5 Projections for the Twenty-First Century. Journal of Climate 26(18) 6859-6881.

Brown, D.G., Verburg, P.H., Pontius, R.G.J, Lange, M.D., 2013. Opportunities to improve impact, integration, and evaluation of land change models. Current Opinion in Environmental Sustainability 5(5) 452-457.

Calvin, K.V., M.A. Wise, L.E. Clarke, J.A. Edmonds, P. Kyle, P.W. Luckow, and A.M. Thomson. 2013. Implications of simultaneously mitigating and adapting to climate change: initial experiments using GCAM. Climatic Change 117 545-560.

Di Vittorio, A.V., Chini, L.P., Bond-Lamberty, B., Mao, J., Shi, X., Truesdale, J., Craig, A., Calvin, K., Jones, A., Collins, W.D., Edmonds, J., Hurtt, G.C., Thornton, P., Thomson, A., 2014. From land use to land cover: restoring the afforestation signal in a coupled integrated assessment-earth system model and the implications for CMIP5 RCP simulations. Biogeosciences 11(22) 6435-6450.

Di Vittorio, A.V., Miller, N.L., 2014. Reducing the impact of model scale on simulated, gridded switchgrass yields. Environmental Modelling & Software 51(0) 70-83.

Dobrowski, S.Z., Abatzoglou, J., Swanson, A.K., Greenberg, J.A., Mynsberge, A.R., Holden, Z.A., Schwartz, M.K., 2013. The climate velocity of the contiguous United States during the 20th century. Global Change Biology 19(1) 241-251.

Eom, J., R.H. Moss, J.A. Edmonds, K.V Calvin, B. Bond-Lamberty, L.E. Clarke, J.J. Dooley, S.H. Kim, R. Kopp, P. Kyle, P.W. Luckow, P.L. Patel, A.M. Thomson, and M.A. Wise. 2012. Scenarios of Future Socio-Economics, Energy, Land Use and Radiative Forcing. In: Engineering Response to Global Climate Change, edited by Robert Watts. CRC Press.

FAO 2016. GAEZ: Global Agro-Ecological Zones. United Nations Food and Agriculture Organization. Available at: http://www.fao.org/nr/gaez/en/.

Fischedick, M., R. Schaeffer, A. Adedoyin, M. Akai, T. Bruckner, L. Clarke, V. Krey, I. Savolainen, S. Teske, D. Ürge-Vorsatz, and R. Wright. Mitigation Potential and Costs. Chapter 10 in O. Edenhofer, R. Pichs-Madruga, Y. Sokona, K. Seyboth, P. Matschoss, S. Kadner, T. Zwickel, P. Eickemeier, G. Hansen, S. Schlömer, and C. von Stechow (eds.) (2011). IPCC Special Report on Renewable Energy Sources and Climate Change Mitigation. Cambridge: Cambridge University Press.

Fischer, G., Shah, M., Tubiello, F.N., van Velhuizen, H., 2005. Socio-economic and climate change impacts on agriculture: an integrated assessment, 1990-2080. Philos Trans R Soc Lond B Biol Sci., 360: 2067–2083.

Fischer, G., van Velthuizen, H.T., 1996. Climate Change and Global Agricultural Potential Project: A Case Study of Kenya. International Institute for Applied Systems Analysis, Laxenburg, Austria, 96 pp.

Fischer, G., van Velthuizen, H., Shah, M., Nachtergaele, F., 2002. Global agro-ecological assessment for agriculture in the 21st century: methodology and results. International Institute for Applied Systems Analysis: Laxenburg, Austria.

Hasegawa, T., Fujimori, S., Takahashi, K., Masui, T., 2015. Scenarios for the risk of hunger in the twenty-first century using shared socioeconomic pathways. Environmental Research Letters 10, 014010.

Haklik, P., Valin, H., Mosnier, A., Obersteiner, M., Baker, J.S., Herrero, M., Rufino, M.C., Schmid, E., 2013. Crop Productivity and the Global Livestock Sector: Implications for Land Use Change and Greenhouse Gas Emissions, American Journal of Agricultural Economics, 95(2) 442-448.

Haxeltine, A., Prentice, I.C., 1996. BIOME3: An equilibrium terrestrial biosphere model based on ecophysiological constraints, resource availability, and competition among plant functional types. Global Biogeochemical Cycles 10(4) 693-709.

Hertel, T., Lee, H., Rose, S.K., Sohngen, B., 2009. Modeling Land-use Related Greenhouse Gas Sources and Sinks and their Mitigation Potential, pp 123-153 in T. Hertel, S.K. Rose, R.S.J. Tol. Economic Analysis of Land Use in Global Climate Change Policy, Routledge.

Hijmans, R.J., Cameron, S.E., Parra, J.L., Jones, P.G., Jarvis, A., 2005. Very high resolution interpolated climate surfaces for global land areas. International Journal of Climatology 25(15) 1965-1978.

Hurtt, G.C., Chini, L.P., Frolking, S., Betts, R.A., Feddema, J., Fischer, G., Fisk, J.P., Hibbard, K., Houghton, R.A., Janetos, A., Jones, C.D., Kindermann, G., Kinoshita, T., Klein Goldewijk, K., Riahi, K., Shevliakova, E., Smith, S., Stehfest, E., Thomson, A., Thornton, P., Vuuren, D.P., Wang, Y.P., 2011. Harmonization of land-use scenarios for the period 1500-2100: 600 years of global gridded annual land-use transitions, wood harvest, and resulting secondary lands. Climatic Change 109(1-2) 117-161.

IIASA/FAO, 2012. Global Agro-ecological Zones (GAEZ v3.0): Model documentation. IIASA, Laxenburg, Austria and FAO, Rome, Italy, pp. 1-179.

IPCC, 2000: Special Report on Emissions Scenarios. A special report of Working Group III [Core Writing Team, N. Nakicenovic and R. Swart (eds.)]. Cambridge University Press, Cambridge, United Kingdom, 608 pp.

IPCC, 2014a: Summary for policymakers. In: Climate Change 2014: Impacts, Adaptation, and Vulnerability. Part A: Global and Sectoral Aspects. Contribution of Working Group II to the Fifth Assessment Report of the Intergovernmental Panel on Climate Change [Field, C.B., V.R. Barros, D.J. Dokken, K.J. Mach, M.D. Mastrandrea, T.E. Bilir, M. Chatterjee, K.L. Ebi, Y.O. Estrada, R.C. Genova, B. Girma, E.S. Kissel, A.N. Levy, S. MacCracken, P.R. Mastrandrea, and L.L. White (eds.)]. Cambridge University Press, Cambridge, United Kingdom and New York, NY, USA, pp. 1-32.

IPCC, 2014b: Climate Change 2014: Synthesis Report. Contribution of Working Groups I, II and III to the Fifth Assessment Report of the Intergovernmental Panel on Climate Change [Core Writing Team, R.K. Pachauri and L.A. Meyer (eds.)]. IPCC, Geneva, Switzerland, 151 pp.

Jones, A.D., Collins, W.D., Edmonds, J., Torn, .S., Janetos, A., Calvin, K.V., Thomson, A., Chini, L.P., Mao, J., Shi, X., Thornton, P., Hurtt, G.C., Wise, M, 2013. Greenhouse Gas Policy Influences Climate via Direct Effects of Land-Use Change. Journal of Climate 26(11) 3657-3670.

Jones, P.G., Thornton, P.K., Heinke, J., 2009. Generating characteristic daily weather data using downscaled climate model data from the IPCC's Fourth Assessment. Waen Associates: Dolgellau, Wales, pp. 1-24.

Kicklighter, D.W., Cai, Y., Zhuang, Q., Parfenova, E.I., Paltsev, S., Sokolov, A.P., Melillo, J.M., Reilly, J.M., Tchebakova, N.M., Lu, X., 2014. Potential influence of climate-induced vegetation shifts on future land use and associated land carbon fluxes in Northern Eurasia. *Environmental Research Letters* 9(3) 035004.

Klein Goldewijk, K., Beusen, A., Janssen, P., 2010. Long-term dynamic modeling of global population and built-up area in a spatially explicit way: HYDE 3.1. The Holocene 20(4) 565-573.

Kyle, P., Luckow, P., Calvin, K., Emanuel, W., Nathan, M., Zhou, Y., 2011. GCAM 3.0 agriculture and land use: Data sources and methods. Report #: PNNL-21025, Pacific Northwest National Laboratory, Richland, WA.

Kyle, P., C. Müller, K. Calvin, and A. Thomson. 2014. Meeting the radiative forcing targets of the representative concentration pathways in a world with agricultural climate impacts. *Earth's Future* 2, 83-98.

Le Quere, C., Andres, R.J., Boden, T., Conway, T., Houghton, R.A., House, J.I., Marland, G., Peters, G.P., van der Werf, G.R., Ahlstrom, A., Andrew, R.M., Bopp, L., Canadell, J.G., Ciais, P., Doney, S.C., Enright, C., Friedlingstein, P., Huntingford, C., Jain, A.K., Jourdain, C., Kato, E., Keeling, R.F., Klein Goldewijk, K., Levis, S., Levy, P., Lomas, M., Poulter, B., Raupach, M.R., Schwinger, J., Sitch, S., Stocker, B.D., Viovy, N., Zaehle, S., Zeng, N., 2013. The global carbon budget 1959-2011. Earth Syst. Sci. Data 5(1) 165-185.

Lee, H.-L., Hertel, T.W., Rose, S., Avetisyan, M. An integrated global land use data base for CGE analysis of climate policy options. Chapter 4, pp. 72-88, in Hertel, T. W., S. Rose and R. Tol (eds.) (2009). Economic Analysis of Land Use in Global Climate Change Policy. Abingdon: Routledge.

Lee, H.-L., Hertel, T.W., Sohngen, B., Ramankutty, N., 2005. Towards an integrated land use database for assessing the potential for greenhouse gas mitigation. Purdue University. GTAP technical paper no. 25, pp. 83.

Loarie, S.R., Duffy, P.B., Hamilton, H., Asner, G.P., Field, C.B., Ackerly, D.D., 2009. The velocity of climate change. Nature 462(7276) 1052-1055.

Masui, T., Matsumoto, K., Hihioka, Y., Kinoshita, T., Nozawa, T., Ishiwatari, S., Kato, E., Shukla, P.R., Yamagata, Y., Kainuma, M., 2011. An emission pathway for stabilization at 6 Wm^{-2} radiative forcing. Climatic Change 109, 59-76.

Maurer, E.P., Adam, J.C., Wood, A.W., 2009. Climate model based consensus on the hydrologic impacts of climate change to the Rio Lempa basin of Central America. Hydrol. Earth Syst. Sci. 13(2) 183-194.

Mearns, L.O., Sain, S., Leung, L.R., Bukovsky, M.S., McGinnis, S., Biner, S., Caya, D., Arritt, R.W., Gutowski, W., Takle, E., Snyder, M., Jones, R.G., Nunes, A.M.B., Tucker, S., Herzmann, D., McDaniel, L., Sloan, L., 2013. Climate change projections of the North American Regional Climate Change Assessment Program (NARCCAP). Climatic Change 120(4) 965-975.

Monfreda, C., Ramankutty, N., Foley, J.A., 2008. Farming the planet: 2. Geographic distribution of crop areas, yields, physiological types, and net primary production in the year 2000. Global Biogeochem. Cycles 22(1) GB1022.

Monfreda, C., Ramankutty, N., Hertel, T. Global agricultural land use data for climate change analysis. Chapter 2, pp. 33-48, in Hertel, T. W., S. Rose and R. Tol (eds.) (2009). Economic Analysis of Land Use in Global Climate Change Policy. Abingdon: Routledge.

Moss, R.H., Edmonds, J.A., Hibbard, K.A., Manning, M.R., Rose, S.K., van Vuuren, D.P., Carter, T.R., Emori, S., Kainuma, M., Kram, T., Meehl, G.A., Mitchell, J.F.B., Nakicenovic, N., Riahi, K., Smith, S.J., Stouffer, R.J., Thomson, A.M., Weyant, J.P., Wilbanks, T.J., 2010. The next generation of scenarios for climate change research and assessment. Nature 463(7282) 747-756.

Müller, C., Robertson, R., 2014. Projecting future crop productivity for global economic modeling. Agricultural Economics 45: 37-50.

Ogle, S.M., Breidt, F.J., Paustian, K., 2006. Bias and variance in model results associated with spatial scaling of measurements for parameterization in regional assessments. Global Change Biology 12(3) 516-523.

Qiao, L., Hong, Y., McPherson, R., Shafer, M., Gade, D., Williams, D., Chen, S., Lilly, D., 2014. Climate Change and Hydrological Response in the Trans-State Oologah Lake Watershed-- Evaluating Dynamically Downscaled NARCCAP and Statistically Downscaled CMIP3 Simulations with VIC Model. Water Resources Management 28(10) 3291-3305.

O'Neill, B.C., Kriegler, E., Ebi, K.L., et al., 2015. The roads ahead: Narratives for shared socioeconomic pathways describing world futures in the 21st century. Global Environmental Change. doi:10.1016/j.gloenvcha.2015.01.004.

O'Neill, B., Kriegler, E., Riahi, K., Ebi, K.L., Hallegatte, S., Carter, T.R., Mathur, R., van Vuuren, D.P., 2014. A new scenario framework for climate change research: the concept of shared socioeconomic pathways. Climatic Change, Special Issue, Nakicenovic N, Lempert R, Janetos A (eds), A Framework for the Development of New Socioeconomic Scenarios for Climate Change Research. doi: 10.1007/s10584-013-0906-1.

Ramankutty, N., Evan, A.T., Monfreda, C., Foley, J.A., 2008. Farming the planet: 1. Geographic distribution of global agricultural lands in the year 2000. Global Biogeochem. Cycles 22(1) GB1003.

Ramankutty, N., Foley, J.A., 1999. Estimating historical changes in global land cover: Croplands from 1700 to 1992. Global Biogeochem. Cycles 13(4) 997-1027.

Reilly, J., Melillo, J., Cai, Y., Kicklighter, D., Gurgel, A., Paltsev, S., Cronin, T., Sololov, A., Schlosser, A., 2012. Using land to mitigate climate change: hitting the target, recognizing the trade-offs. *Environmental Science & Technology* 46(11), 5672-5679.

Riahi, K., Rao, S., Krey, V., Cho, C., Chirkov, V., Fischer, G., Kindermann, G., Nakicenovic, N., Rafaj, P., 2011. RCP 8.5—A scenario of comparatively high greenhouse gas emissions. Climatic Change 109, 33-57.

Riley, W.J., Biraud, S.C., Torn, M.S., Fischer, M.L., Billesbach, D.P., Berry, J.A., 2009. Regional CO2 and latent heat surface fluxes in the Southern Great Plains: Measurements, modeling, and scaling. J. Geophys. Res. 114(G4) G04009.

Roeckner, E., Arpe, K., Bengtsson, L., Christoph, M., Claussen, M., Dumenil, L., Esch, M., Giorgetta, M., Schlese, U., Schulzweida, U., 1996. The atmospheric general circulation model ECHAM4: Model description and simulation of present day climate. Max Planck Institute for Meteorology: Hamburg, Germany, pp. 1-90.

Roeckner, E., Bauml, G., Bonaventura, L., Brokopf, R., Esch, M., Giorgetta, M., Hagemann, S., Kirchner, I., Kornblueh, L., Manzini, E., Rhodin, A., Schlese, U., Schulzweida, U., Tompkins, A., 2003. The atmospheric general circulation model ECHAM5 part I. Max Planck Institute for Meteorolgy: Hamburg, Germany, pp. 1-127.

Rosegrant, M.W., and IMPACT Development Team, 2012. International Model for Policy Analysis of Agricultural Commodities and Trade (IMPACT) Model Description. International Food Policy Research Institute, Washington, D.C.

Sands, R., Schumacher, K., Forster, H., 2014. U.S. CO2 mitigation in a global context: welfare, trade, and land use. The Energy Journal 35 SI1, 181-197.

Schmitz, C., van Meijl, H., Kyle, P., Nelson, G.C., Fujimori, S., Gurgel, A., Havlik, P., Heyhoe, E., d'Croz, D.M., Popp, A., Sands, R., Tabeau, A., van der Mensbrugghe, D., von Lampe, M., Wise, M., Blanc, E., Hasegawa, T., Kavallari, A., Valin, H., 2014. Land-use change trajectories up to 2050: insights from a global agro-economic model comparison. Agricultural Economics, 45(1) 69-84.

Searle, S., Malins, C., 2015. A reassessment of global bioenergy potential in 2050. GCB Bioenergy 7(2) 328-336.

Snell, R.S., Huth, A., Nabel, J.E.M.S., Bocedi, G., Travis, J.M.J., Gravel, D., Bugmann, H., Gutiérrez, A.G., Hickler, T., Higgins, S.I., Reineking, B., Scherstjanoi, M., Zurbriggen, N., Lischke, H., 2014. Using dynamic vegetation models to simulate plant range shifts. Ecography 37(12) 1184-1197.

Sohngen, B., Mendelsohn, R., Sedjo, R., 1999. Forest Management, Conservation, and Global Timber Markets. American Journal of Agricultural Economics 81(1) 1-13.

Taylor, K.E., Stouffer, R.J., Meehl, G.A., 2012. An Overview of CMIP5 and the Experiment Design. Bulletin of the American Meteorological Society 93(4) 485-498.

Thomson, A.M., Calvin, K.V., Smith, S.J., Kyle, G.P., Volke, A., Patel, P., Delgado-Arias, S., Bond-Lamberty, B., Wise, M.A., Clarke, L.E., Edmonds, J.A., 2011. RCP4.5: A pathway for stabilization of radiative forcing by 2100. Climatic Change 109, 77-94.

van der Linden, P. and Mitchell, J.F.B. (eds.) 2009: ENSEMBLES: Climate Change and its Impacts: Summary of research and results from the ENSEMBLES project. Met Office Hadley Centre, FitzRoy Road, Exeter EX1 3PB, UK. 160pp.

van Vuuren, D., Edmonds, J., Kainuma, M., Riahi, K., Thomson, A., Hibbard, K., Hurtt, G., Kram, T., Krey, V., Lamarque, J.-F., Masui, T., Meinshausen, M., Nakicenovic, N., Smith, S., Rose, S., 2011a. The representative concentration pathways: an overview. Climatic Change 109(1-2) 5-31.

van Vuuren, D.P., Kriegler, E., O'Neill, B.C., Ebi, K.L., Riahi, K., Carter, T.R., Edmonds, J., Hallegatte, S., Kram, T., Mathur, R., Winkler, H., 2013. A new scenario framework for Climate Change Research: scenario matrix architecture. Climatic Change, 122(3) 373-386.

van Vuuren, D.P., Stehfest, E., den Elzen, M.G.J., Kram, T., van Vliet, J., Deetman, S., Isaac, M., Klein Goldewijk, K., Hof, A., Mendoza Beltran, A., Oostenrijk, R., van Ruijven, B., 2011b. RCP2.6: Exporing the possibility to keep global mean temperature increase below 2°C. Climatic Change 109, 95-116.

Verburg, P.H., Mertz, Ol, Erb, K.-H., Haberl, H., Wu, W., 2013. Land system change and food security: towards multi-scale land system solutions. Current Opinion in Environmental Sustainability 5(5) 494-502.

Von Lampe, M., Willenbockel, D., Ahammad, H., et al., 2014. Why do global long-term scenarios for agriculture differ? An overview of the AgMIP Global Economic Model Intercomparison. Agricultural Economics 45: 3-20.

Wilkenskjeld, S., Kloster, S., Pongratz, J., Raddatz, T., Reick, C.H., 2014. Comparing the influence of net and gross anthropogenic land-use and land-cover changes on the carbon cycle in the MPI-ESM. Biogeosciences 11(17) 4817-4828.